

2 **Relic Groundwater and Mega Drought Confound Interpretations of Water**
3 **Sustainability and Lithium Extraction in Arid Lands**

4 Brendan J. Moran¹ 0000-0002-9862-6241, David F. Boutt¹ 0000-0003-1397-0279, Sarah V.
5 McKnight¹ 0000-0002-6013-193X, Jordan Jenckes² 0000-0002-1811-3076, Lee Ann Munk²
6 0000-0003-2850-545X, Daniel Corkran¹ 0000-0001-6168-8281, Alexander Kirshen¹ 0000-0003-
7 2015-4085

8 ¹Department of Geosciences, University of Massachusetts Amherst

9 ²Department of Geological Sciences, University of Alaska Anchorage

10 Corresponding author: Brendan Moran, bmoran@geo.umass.edu

11 **Keywords:** Salar de Atacama, Chile; Tritium; Groundwater Sustainability; Hydroclimate; Water
12 Budget; Lithium Brine

13 **Key Points:**

- 14 • Freshwater inflows and the modern water budget at Salar de Atacama are dominated by
15 relic groundwater.
- 16 • A long-term mega drought coincident with increases in groundwater extraction
17 complicates the attribution of specific anthropogenic environmental impacts.
- 18 • Freshwater use and allocated water rights at the Salar de Atacama appear to not meet
19 sustainable metrics.

21 **Abstract**

22 Demand for lithium for batteries is growing rapidly with the global push to decarbonize
23 energy systems. The Salar de Atacama, Chile holds ~42% of the planet’s reserves in the form of
24 brines hosted in massive evaporite aquifers. The mining of these brines and associated freshwater
25 use has raised concerns over the sustainability of lithium extraction, yet large uncertainties
26 remain regarding fundamental aspects of governing hydrological processes in these
27 environments. This incomplete understanding has led to the perpetuation of misconceptions
28 about what constitutes sustainable or renewable water use and therefore what justifies
29 responsible allocation. We present an integrated hydrological assessment using tritium and stable
30 oxygen & hydrogen isotopes paired with remotely sensed and terrestrial hydroclimate data to
31 define unique sources of water distinguished by their residence time, physical characteristics, and
32 connectivity to modern climate. Our results describe the impacts of major drought on surface and
33 groundwaters and demonstrate that nearly all inflow to the basin is composed of water recharged
34 >65 years ago. Still, modern precipitation is critical to sustaining important wetlands around the
35 salar. Recent large rain events have increased surface water and vegetation extents and terrestrial
36 water storage while mining-related water withdrawals have continued. As we show in this basin,
37 poor conceptualizations of these complex hydrological systems have perpetuated the
38 misallocation of water and the misattribution of impacts. These fundamental issues apply to
39 many similar regions globally. Our new framework for hydrological assessment in these arid
40 basins moves beyond calculating gross inputs-outputs at a steady-state to include all
41 compartmentalized stores that constitute “modern” budgets.

42 **Plain Language Summary**

43 Lithium is a critical resource for the green energy transition as the primary component in
44 lithium-ion batteries. Most of the planet’s resources occur in dry, water-scarce environments,
45 like Salar de Atacama in Chile, where ~42% of the world’s supply exists. The lithium resides in
46 very salty groundwater (brine) beneath its salt flat. Large amounts of brine along with some
47 freshwater are extracted to recover lithium, and as the world requires more, there is increasing
48 scrutiny of water use and resulting environmental impacts. Yet, persistent gaps remain regarding
49 our fundamental understanding of how and where water moves in these environments and
50 therefore the impacts that its extraction may have on surrounding ecosystems and communities.

51 We employ a combination of satellite and ground-based hydrological and climatological data
52 paired with water isotopes to comprehensively assess changes in the distribution and movement
53 of groundwater and surface waters. Our results show that a major drought and subsequent wetter
54 period are the primary drivers of surface hydrology changes over this period. We also show that
55 most of the water here is very old, highlighting the shortcomings of current water allocations in
56 the region, which assume that most of the water in the system is relatively young. This work
57 presents a data-driven framework that for the first time allows water sustainability and lithium
58 extraction to be adequately assessed in these arid regions.

59 **1. Introduction**

60 Water allocation and consumption are at the center of the debate surrounding resource
61 extraction in many watersheds globally (Boulay et al., 2018; Pfister et al., 2009; Ridoutt &
62 Pfister, 2010; Wada et al., 2017; Zipper et al., 2020). In particular, the extraction of lithium
63 brines and associated freshwater use in arid regions have recently drawn the attention of many
64 stakeholders seeking to understand the environmental impacts of the transition to green energy
65 along the lithium-ion battery supply chain (Gajardo & Redón, 2019; Gutiérrez et al., 2018;
66 Sonter et al., 2020). Lithium mining has a remarkably spatially explicit water scarcity footprint
67 (Schomberg et al., 2021) because exploited deposits have a strong connection to climate aridity
68 (Munk et al., 2016). In northern Chile, which globally has the largest lithium reserve (Munk et
69 al., 2016), fresh groundwater has reached unprecedented demand and market prices (Oyarzún &
70 Oyarzún, 2011). Yet for the Salar de Atacama (SdA), which represents the largest single
71 recoverable lithium resource in the world with approximately 42% of the global reserve base as
72 of 2021 (Cabello, 2021, USGS, 2022), no studies to date have constrained the capability of the
73 basin's water budget to meet current water demands, possibly because of notable uncertainty
74 between permitted water use and actual extraction (Babidge et al., 2019), and the lack of
75 legitimate sustainability metrics. Rapidly increasing global demand for lithium (Kesler et al.,
76 2012; Ambrose and Kendall, 2020) coupled with the hydrologic imbalance between recharge and
77 discharge in this basin (Boutt et al., 2021) therefore necessitates a critical examination of water
78 sustainability in light of anthropogenic and climatic pressures on these environments.

79 Human activities including mineral resource extraction and other water consumption
80 (irrigation, domestic use) have large impacts on the water budgets of basins (AghaKouchak et

81 al., 2021; Wang et al., 2018). In arid environments especially, attribution of hydrologic impacts
82 from such activities can be difficult due to large interannual precipitation variability and the lack
83 of long-term, continuous instrumental records (Ashraf et al., 2021; Bierkens & Wada, 2019;
84 Rivera et al., 2021). Changes in rainfall patterns and timing lead to complex fluctuations in
85 surface water features and water table positions (Fan et al., 2013). Yet the common practice of
86 monitoring for mining purposes consists of baseline measurements that are only collected for a
87 few years before the start of projects and therefore do not allow for the assessment of the natural
88 variability of hydrologic systems. Furthermore, the over-reliance on steady-state water budget
89 accounting for management, rather than focusing on the specific inventory of water resources has
90 resulted in substantial misunderstandings of these systems (McDonnell, 2017).

91 The importance of highly variable precipitation events and the small margin for error in
92 water-limited environments makes it challenging to responsibly allocate water resources in these
93 basins (Stonestrom & Harrill, 2007; Schaffer et al., 2019; Somers & McKenzie, 2020). Pluvial
94 events and droughts along with their timing have strong control on the inferred hydrologic
95 conditions of a particular watershed and water allocation (Houston & Hart, 2004; Ferrero &
96 Villalba, 2019). Reliance on outmoded methods of accounting by the water authorities in SdA, in
97 particular, evokes questions of whether water allocations have ever met sustainable metrics
98 (Bredehoeft, 2002). Having a data-driven and justifiable scientific understanding of the
99 hydrological regime is key to avoiding mistakes in system conceptualization, water allocation,
100 and the propagation of misinformation in the public domain.

101 In these arid environments surface water discharge is dominated by either infrequent
102 precipitation events, seasonal snowmelt runoff, or spring discharge and stream baseflow fed by
103 groundwater (Masbruch et al., 2016). These three sources of water can have very different
104 residence times and respond distinctly to changes in hydrological conditions. In addition, long-
105 term aridity develops deep water tables and long flow paths, creating effective catchment areas
106 that are often much larger than topographic watersheds (Liu et al., 2020; Gleeson et al., 2011).
107 The groundwater near basin floors, therefore, tends to be dominated by long transit times
108 (Schaller & Fan, 2009). The resulting surface and groundwater bodies in these systems can
109 display substantial variability in source water and responses to perturbations over relatively small
110 spatial scales. Understanding how different water compartments respond to interannual
111 hydrological variability is therefore critical to resource understanding and management.

112 The work presented here integrates remotely sensed and ground-based climate data,
113 physical hydrological assessments, and tritium-based residence time analyses to determine
114 changes in water storage and fluxes in the SdA catchment. We document that the region has
115 experienced major paleo-hydrological changes in the past that left behind relic (premodern or
116 fossil) waters, which naturally sustain modern wetland complexes but are being exploited for
117 industrial use. We show that over the last two decades a region-wide Mega Drought has further
118 impacted water availability concomitant with increased water use and resource extraction
119 (Garreaud et al., 2020). In more recent years, a shift to wetter and more variable conditions has,
120 in fact, increased total basin water storage and expanded many natural surface water features.
121 Clear assessments and attribution of impacts are challenging because of the confounding nature
122 of climate variability and human water use but are essential to evaluating the sustainability of
123 lithium resource devolvement.

124 **2. Background**

125 **2.1. Climate**

126 The SdA basin lies within the Preandean Depression at the margin of the hyperarid
127 Atacama Desert core to the west, and the Western Cordillera and Altiplano-Puna Plateau to the
128 east. The region surrounding the basin has become known as the Lithium Triangle as it contains
129 most of the world's lithium resources (**Figure 1a**). Annual precipitation west of the Andes
130 including the floor of SdA averages only 2-15 mm/year, while many areas above 4,500 masl can
131 average 250-300 mm/year (DGA, 2013; Houston, 2006). Of this high-elevation precipitation,
132 approximately 50 to 80 mm of snow water equivalent falls each year; however, much of this
133 liquid sublimates or evaporates before infiltrating due to high insolation and low relative
134 humidity (Vuille & Ammann, 1997; Kinnard et al., 2020). Recent evidence indicates that this
135 dry-season snowfall has decreased by ~10% per decade since the 1980s (Cordero et al., 2019).
136 Most of the annual precipitation in the basin (>80%) occurs in summer, from December through
137 March, and is inherently episodic, occurring in clusters of about a week when large amounts of
138 rainfall can occur over short periods (Garreaud et al., 2003; Valdivielso et al., 2020). The
139 condensed and convective nature of rainfall means that annual totals can significantly vary year-
140 to-year, especially at lower elevations (Garreaud et al., 2003). Widespread diffuse recharge likely

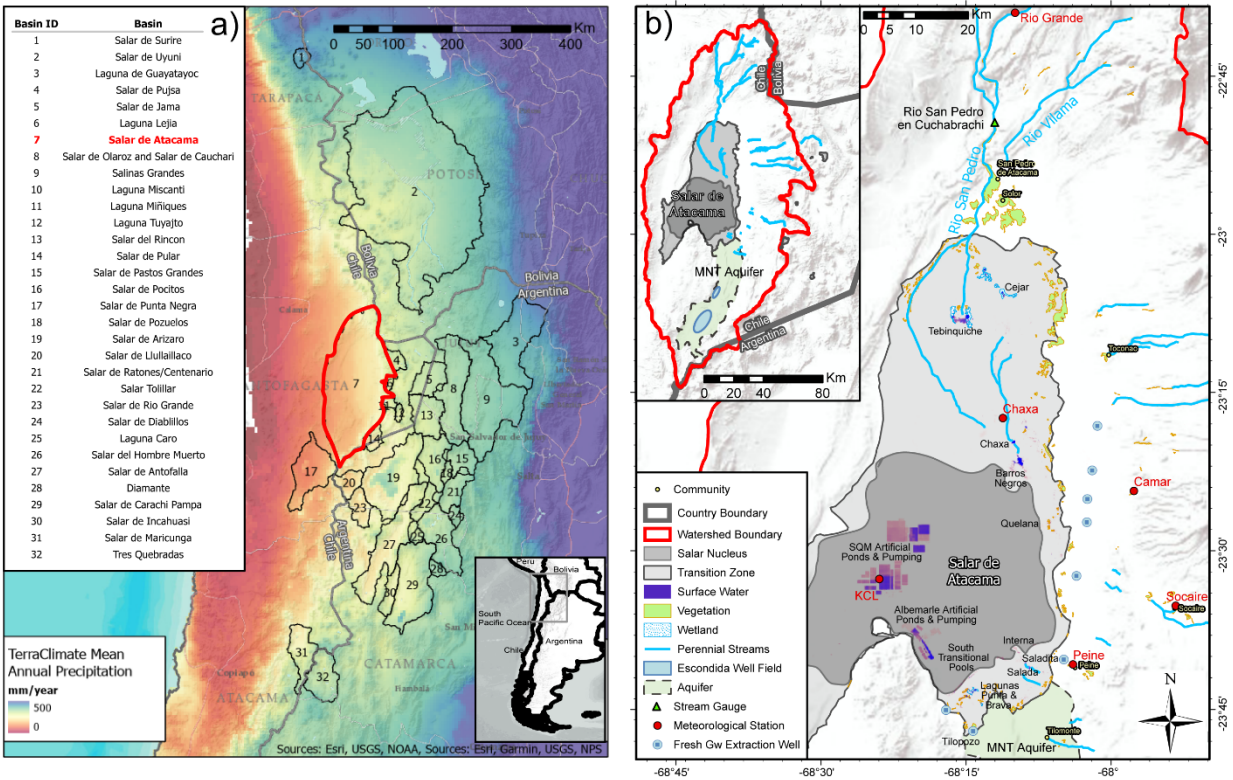


Figure 1. Major lithium-bearing basins of the Dry Andean Plateau of South America. **(a)** The regional mean annual precipitation of the region and the SdA basin topographic watershed are outlined in red. **(b)** Inset map of the SdA basin and its hydrological features. The salar nucleus, transition zone, surface waters, vegetated wetlands, and perennial streams are outlined. Meteorological stations and the stream gauge are labeled along with the location of fresh groundwater extraction wells. The MNT aquifer is highlighted in green, and streams (rivers) are in blue.

141 only occurs at elevations above ~3,900 masl where rainfall surpasses known thresholds required
 142 for recharge (e.g., Scanlon et al., 2006; Houston, 2007, 2009; Boutt et al., 2016). However,
 143 infrequent high-intensity rainfall events likely produce focused surface flows and groundwater
 144 recharge in parts of the basin (Houston, 2006; Boutt et al., 2016). No permanent ice exists at
 145 present within the recharge area of SdA except for some localized rock glaciers that may be
 146 present above 4,500 masl (Schaffer et al., 2019; Jones et al., 2019).

147 Paleoclimate records in the region indicate that hyperarid to arid climates dominated for
 148 at least the past 53 ka (Bobst et al. 2001; Godfrey et al. 2003), with at least four periods wetter
 149 than the modern occurring since 106 ka (Gayo et al. 2012). The most recent of these pluvial
 150 periods, around the last glacial maximum, increased precipitation by 2-3 times modern amounts
 151 and lasted for several thousand years (Placzek et al. 2013). Records from multiple Altiplano
 152 lakes indicate lake levels increased by tens of meters during this period (Blard et al., 2011), and

153 Laguna Lejía approximately 40 km east of the salar at 4,325 masl was ~25 m higher than today,
154 which would require double the modern precipitation rate, up to 500 mm/year (Grosjean et al.,
155 1995; Grosjean & Núñez, 1994). The climate around SdA has been drier since the mid-Holocene
156 based on evidence that water tables were below the ground surface at paleo-wetland sites and
157 observations from sediment cores from the salar nucleus (Rech et al. 2003; Quade et al. 2008;
158 Placzek et al. 2013). These wet periods dramatically altered the hydrological and ecological
159 conditions in the basin (Pfeiffer et al., 2018), and the effects are likely still evident in the modern
160 hydrological system in the form of transient groundwater storage changes within the deep and
161 extensive regional aquifers responding over 100-10,000-year time scales (Moran et. al., 2019).

162 **2.2. Basin Hydrology**

163 The SdA basin catchment is a large and deep topographic depression of about 17,000 km²
164 that spans a vertical profile of >3500 meters, its basin floor (2,900 km²) is covered mostly by
165 evaporite sediments with some clastic material and hosts a vast halite nucleus covering about
166 1,700 km². The water budget and physical hydrology of the SdA region have been the focus of
167 several recent studies (Houston, 2007, Corenthal et al., 2016, Munk et al., 2018, Boutt et al.,
168 2021). A summary of the key hydrological attributes at SdA is introduced here (**Figure 1b**). Due
169 to the extreme aridity, there is only one river (Rio San Pedro) that directly feeds the floor of the
170 basin, while several smaller streams infiltrate completely before reaching the basin floor. About
171 2/3's of inflow to the basin is from low to mid-elevation (~2,450-2,600 masl) spring-fed streams
172 and diffuse groundwater inflow through tabular ignimbrite sheets and alluvial fans. These
173 inflows that discharge above the basin floor re-infiltrate into the permeable alluvial fan deposits
174 before at least some portion emerges again as springs near the salar floor. Water leaves the basin
175 through direct evaporation (and limited transpiration) in marginal areas herein called transition
176 zones. The intense evaporation that far outpaces precipitation on the basin floor has created a
177 massive evaporite deposit (Corenthal et al., 2016) and brine body. The high-density brine
178 interacts with inflowing freshwater to create density-driven groundwater flow conditions and
179 fresh groundwater upwelling, which in turn results in freshwater discharge from the low
180 elevation springs (McKnight et al., 2021). The halite-rich brine aquifer, within the nucleus, is
181 currently being exploited for its lithium resource (Munk et al., 2016). Geochemical evidence and
182 physical hydrogeological conceptualization (Munk et al., 2021) do not support a source of

183 modern groundwater inflow to the brine aquifer, while Boutt et al. (2016) document recharge to
184 the brine body through direct precipitation and infiltration of surface waters that accumulate
185 along the halite nucleus margin.

186 In a recent contribution, Boutt et al. (2021) presented a comprehensive review of the
187 water budget and discussed different conceptualizations of basin hydrology. They show that the
188 amount of observed water inflow to the basin floor is a large percentage (~25%) of estimated
189 total modern precipitation inputs. Basin yields approaching even 4-8% of the total precipitation
190 are not realistic in arid environments with deep water tables, thick vadose zones, and large
191 evaporative demands (Scanlon et al., 2002). Following Corenthal et al. (2016) that showed the
192 annual modern hydrologic budget within the topographic watershed does not close and
193 implicated interbasin groundwater flow and relic or “fossil” water inflows to close the budget,
194 Moran et al. (2019) provided geochemical and hydrophysical evidence to support this
195 conclusion. Regardless of the mechanism invoked to balance the budget, these results
196 significantly impact how the basin water budget must be treated and managed.

197 **2.3. Water Use**

198 Water use in SdA has a long history that originates with indigenous communities, known
199 as the Atacameños, who have been using surface waters for agriculture and domestic uses for
200 millennia (Babidge et al., 2019). Only in the past three decades has water been managed by the
201 national governing agency known as Dirección General de Aguas (DGA) as groundwater
202 extraction for mining purposes increased (Anderson et al., 2002). During that period, allocated
203 water rights by the DGA resulted in the development of groundwater extraction wells. Before
204 this, water was primarily consumed from perennial streams and springs at the surface and almost
205 all non-industrial water use is still from these surface water sources. Water consumption
206 currently serves diverse purposes in the basin, including mining, agricultural, and domestic use
207 (DGA, 2013; Babidge, 2019). The understanding of actual consumption is limited to reported
208 pumping rates from industrial users and poorly constrained estimates of non-industrial use
209 (AMPHOS21, 2018). Thus, as we further show in this study, understanding water use is limited
210 to what is reported and permitted, and may not fully encompass total water use occurring in the
211 basin. Nevertheless, with currently available water use estimations, there exists no meaningful

212 analysis of whether this water use can be considered sustainable within the current water budget
213 framework.

214 **3. Methods and Approach**

215 **3.1. Remote Sensing**

216 This study utilizes multiple remotely sensed data sets to assess the recent hydrological
217 and climatological regimes at SdA. These include Landsat satellite imagery (spatial resolution of
218 30 meters with imagery every ~16 days), TerraClimate climatically-aided interpolation of
219 precipitation, and the Gravity Recovery & Climate Experiment (GRACE). To extract long-term
220 seasonal time series of surface water extent we utilized the Joint Research Centre (JRC) global
221 monthly water extent imagery (Pekel et al., 2016). Using GEE, we extracted a full series of
222 images from Landsat 5 & 7 Surface Reflectance Tier 1 (atmospherically corrected ETM sensor)
223 data for 1984 through 2020 and determined the number of pixels covered by vegetation from
224 which a total geographic area was calculated using a set of off-the-shelf functions provided by
225 the GEE API. This provides a time series of the total area covered by living or “green”
226 vegetation within the ROI. Further description of these methods and analysis of the reliability of
227 the TerraClimate dataset relative to other data products is included in the supplemental material
228 (**Text S1**).

229 To extend our hydroclimatic assessment we utilized data from GRACE which provides
230 Terrestrial Water Storage Anomaly (TWSA) at a monthly resolution based on small changes in
231 Earth’s gravity field. The spatial resolution of the dataset is coarse (3.0° downscaled to 0.5°) but
232 is an excellent tool for assessing changes in total water storage at the basin scale (Reager et al.,
233 2013). Time series of TWSA (relative to a 2004-2009 baseline), presented as a liquid water
234 equivalent thickness, were produced for the SdA basin from monthly mass grids produced by
235 two centers: CSR (university of Texas/Center for Space Research) and JPL (NASA Jet
236 Propulsion Laboratory) publicly available from GRACE Tellus
237 (<https://grace.jpl.nasa.gov/data/get-data/>; Landerer, 2021).

238 3.2. Terrestrial Groundwater, Surface Water, and Precipitation Data

239 This study utilizes streamflow, precipitation, and groundwater level measurements from
240 locations throughout the SdA catchment to assess changes in hydrologic conditions. We obtained
241 streamflow records from the Rio San Pedro en Cuchabrachi stream gauge and precipitation
242 records for the Camar, Peine, Rio Grande, and Socaire meteorological stations from the DGA
243 (<https://snia.mop.gob.cl/BNAConsultas/reportes>) (**Figure 1b**). Additional precipitation records
244 for the Chaxa and KCL meteorological stations came from the Sociedad Quimica y Minera S.A.
245 (SQM) environmental monitoring database (<https://www.sqmsenlinea.com/meteorology>).

246 3.3. Water Residence Times

247 To assess spatially explicit water residence times within the hydrological system we
248 utilize stable ($\delta^{18}\text{O}$ & $\delta^2\text{H}$) and radiogenic (^3H) isotopic tracers, along with dissolved chloride
249 (Cl^-) in 106 water samples across the SdA catchment. These include surface and groundwaters
250 collected during numerous field campaigns between October 2011 and March 2021. Samples
251 were collected with a consistent, standardized procedure and in-situ measurements of
252 temperature, specific conductance, and pH were made at each sampling location during
253 collection. These data are presented in full in the supplemental material (**Table S1**) and a
254 detailed analytical procedure is also provided (**Text S1**).

255 *Physical Water Type Classification*

256 Sampled waters were grouped into seven physical water types to facilitate the
257 interpretation and communication of our results. These distinctions are based on extensive
258 knowledge of the regional hydrogeology gathered during more than ten field campaigns,
259 previously published works, and scrutiny of geochemical signatures (Munk et al., 2021). Nucleus
260 Brines are groundwaters from the core of the halite-dominated brine aquifer, sampled at shallow
261 depths <13 meters below ground level (mbgl), Marginal Brines are groundwaters from the
262 margins of the brine aquifer, sampled at the water table (<2 mbgl). Transitional Pools are highly
263 saline, shallow pools that form at the margin of the halite crust which grow and shrink rapidly
264 primarily in response to precipitation events. These are often adjacent to (~1-2km away) but
265 distinct from the Lagoons which include the culturally and ecologically important lagoons Brava,

266 Chaxa, and Tebinquiche. Many of these water bodies also grow and shrink seasonally and after
267 precipitation events but are perennially extant. They are also quite shallow (<1m) but much less
268 saline than the Transitional Pools. The basin inflow waters are separated into three groups;
269 Streams are perennially flowing fresh surface waters, Inflow Groundwaters (Inflow Gw) are
270 fresh to brackish waters sampled from wells upgradient of the salar transition zone, and
271 Transition Zone Groundwaters are brackish to saline waters sampled at the water table within the
272 salar transition zone.

273 *Tritium Age Tracing Approach*

274 The hydrological system at SdA is complex and heterogeneous on all scales, and large
275 gaps exist in hydrogeological and hydroclimatological data coverage especially above the basin
276 floor and on the adjacent plateau. Very deep water tables and rugged terrain make direct
277 observation of the groundwater system impractical across much of the landscape, and long-term
278 high-quality terrestrial monitoring of the hydroclimate is sparse. Therefore, highly parameterized
279 models and tracers that require additional assumptions are not the most effective tools in this
280 environment. Tracing the water molecule itself most accurately integrates small-scale variability
281 with large-scale processes (Birkel et al., 2015; Buttle, 1994). Stable isotope ratios ($\delta^{18}\text{O}$, $\delta^2\text{H}$)
282 and radioisotopes (^3H) in water offer many unique advantages in these systems (Cook & Bohlke,
283 2000; Kendall & Caldwell, 1998). Signatures of $\delta^{18}\text{O}$ & $\delta^2\text{H}$ in groundwater remain unchanged
284 from the point of recharge until its re-emergence from the ground (Beria et al., 2018; Clark &
285 Fritz, 1997; Kendall & McDonnell, 1998). Radioisotope signatures (^3H) are also conservative in
286 this way but also follow a predictable decay (half-life of 12.32 years) during transit. To
287 effectively utilize this tracer, we must constrain the ^3H content of modern precipitation as the
288 modern recharge signature for inflows. This value, also presented by Boutt et al. (2016) and
289 Moran et al. (2019), is determined to be 3.23 ± 0.6 TU (1σ) from five carefully chosen, amount
290 weighted rain samples collected during 2013 and 2014. This value is within the range reported
291 by others in the region (Cortecci et al., 2005; Grosjean et al., 1995; Herrera et al., 2016; Houston,
292 2002, 2007).

293 Widespread atmospheric nuclear bomb testing in the late 1950s and early '60s created a
294 large and unmistakable peak in global atmospheric ^3H concentrations which increased

295 concentrations in meteoric water globally by greater than an order of magnitude (Cartwright et
296 al., 2017). This unmistakable signature allows for reliable differentiation between water
297 recharged post-1955 and that emplaced before. We assume the modern value in meteoric water
298 described above is representative of average precipitation from about 2000 to the present since
299 the bomb peak signature is no longer resolvable after that date in the Southern Hemisphere
300 (Rooyen et al., 2021). This background signature should also be representative of precipitation
301 before the mid-1950s since the bomb peak had not yet occurred (Houston, 2007; Jasechko,
302 2016). Since the ^3H activity in any given sample is a bulk sample representing mixtures of
303 unknown sources and respective amounts, we must be careful not to over-interpret specific ^3H
304 activity values in individual samples. To ensure reliable and conservative interpretation we
305 determine a “percent modern water” ratio in each sample as the ratio of background meteoric
306 input activity to the activity measured in the sample. In this extreme, arid environment
307 essentially all water reliably contains either very small amounts of measurable ^3H (<0.15 TU) or
308 a substantial amount (>1.0 TU). Water recharged in 1955 before the bomb peak with a ^3H
309 content of 3.23 ± 0.6 TU would have between 0.08 and 0.11 TU in July 2018, or 2-3% of the
310 meteoric input value (Stewart et al., 2017). Due to the small but non-negligible analytical
311 uncertainty (~ 0.02 - 0.07 TU at low activities) and potential very low levels of in-situ creation of
312 ^3H , samples with these very small activities are herein considered to be effectively ^3H -dead
313 waters or indistinguishable from zero. Waters registering such low activities are assumed to
314 contain negligible volumes of water recharged post-bomb peak (1955), as even small amounts of
315 water with higher activities would readily skew total activities in these ^3H -dead samples to an
316 observable effect. Since most of the waters measured in this environment contain effectively no
317 ^3H , our objective is not to directly estimate discrete mean residence time distributions but instead
318 to describe the relative proportions of ^3H -dead to recent recharge (<65 years old) in these waters
319 (Cartwright et al., 2017). This relative water age value allows for the reliable interpretation of
320 connections to modern meteoric inputs, as well as the lack thereof.

321 **3.4. Water Use Quantification**

322 We compiled all available water use data within the SdA basin to develop a
323 comprehensive basin-wide assessment of anthropogenic water use. The DGA maintains and
324 publishes a national database of all water use permits in Chile. Several public reports analyzing

325 resource and reserve estimates of lithium have used this database to analyze possible impacts of
326 water use (AMPHOS21, 2018). We utilize this DGA database along with communications with
327 local communities to present and assess total freshwater allocation in SdA. To calculate
328 estimated actual freshwater use in the basin, we used groundwater pumping rates from mining
329 companies, available in public reports. A detailed description of how these data were collected is
330 given in the supplemental material (**Text S1**)

331 **4. Results**

332 **4.1. Climate, Hydrology, and Water Storage Changes**

333 *Precipitation*

334 We characterize the climate regime at SdA since 1984 using the TerraClimate dataset and
335 station-based meteorological data from the six longest and most complete records, identifying
336 several distinct periods including two long-term droughts and three wet intervals (**Figure 2**). To
337 properly frame these results, it's important to point out distinctions between the instrumental and
338 remotely sensed records. First, TerraClimate represents an area-integrated mean annual
339 accumulation value for the entire SdA topographic watershed, including the basin floor (~20% of
340 the watershed area) which averages <15 mm/year. These data provide a reliable assessment of
341 basin-scale climate and multi-annual trends but naturally smooth large interannual and spatial
342 variations in precipitation. For instance, the SdA mean annual precipitation in the TerraClimate
343 record (1958-2020) is 37 mm/year with a standard deviation of 18mm (**Figure 2b**). The longest
344 and most complete record in the basin, Camar station (1979-2019) located about 400 meters
345 above the basin floor recorded a mean of 43 mm/year with a standard deviation of 46 mm
346 (**Figure 2a**). The interannual variability is larger than the mean annual precipitation at Camar, a
347 feature common among station records in the basin. This basin spans about 150 km from north to
348 south, thus precipitation at Rio Grande station near the northern end is consistently greater than
349 at Socaire station in the southern part of the basin even though they are at the same elevation.
350 The climate intervals presented here are intended to describe overall changes by correlating
351 station data trends and basin-wide average amounts, but it's important to recognize that the
352 timing and magnitude of these changes vary across the basin.

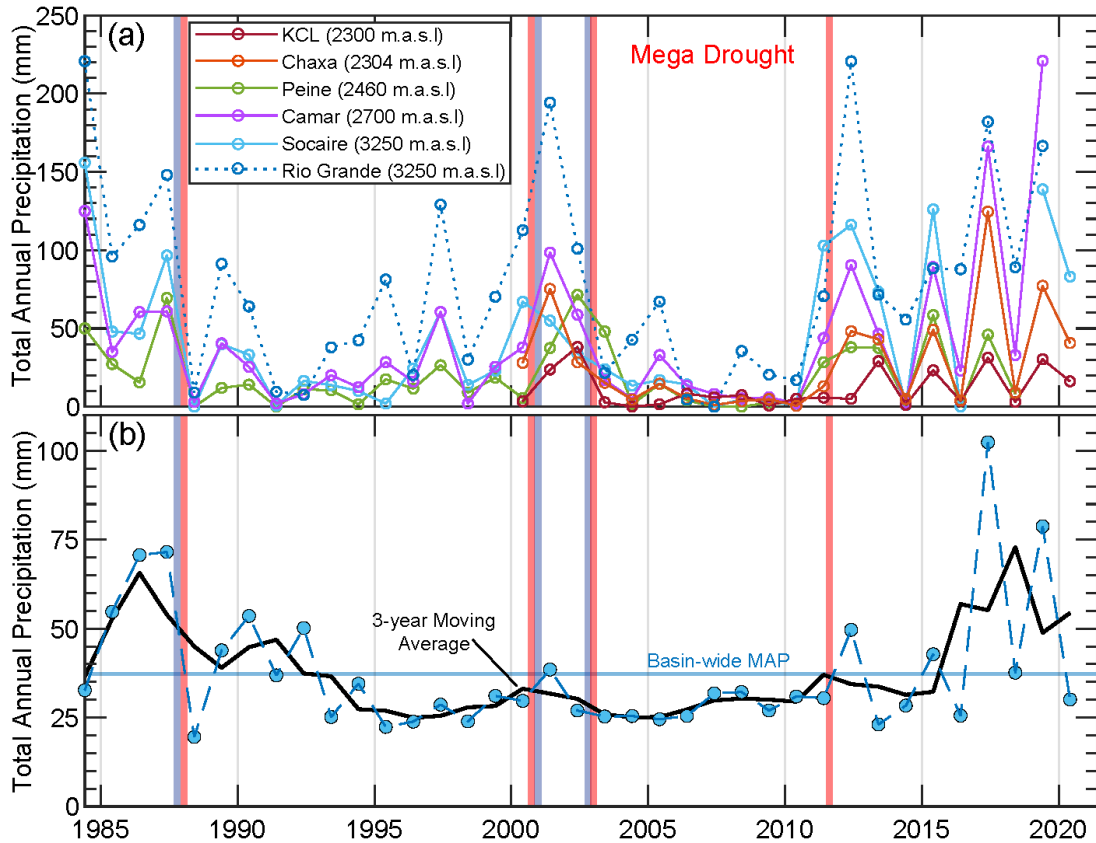


Figure 2. Annual precipitation from 1984-2020. Vertical red/blue bars represent major climate intervals identified. **(a)** Shows records from meteorological stations within the basin, the Rio Grande station record is a dotted line due to its location at the northern end of the basin. **(b)** The basin-wide area-integrated annual precipitation from the TerraClimate dataset with the 3-year moving average. The Mean Annual Precipitation (MAP) from the TerraClimate record (1958-present) is indicated by the blue horizontal line.

353 Localized and interannual variations are captured by station data; however, large events
 354 can be recorded at certain stations and barely register at others or occur several weeks apart. For
 355 instance, February-March of 2001 was one of the wettest periods on record in the north and
 356 northeast of the basin where Rio Grande (178mm), Chaxa (71 mm), and Camar (99mm) all
 357 recorded greater than double their mean annual precipitation in just a few weeks. The stations in
 358 the south and east recorded average or below-average precipitation that year, however, the
 359 following year Peine and KCL stations had their wettest year on record. When interpreting
 360 hydroclimate changes and their responses basin-wide we need to account for these spatial
 361 differences as well as the overall regime. Therefore, we define major long-term intervals and
 362 individual events that are registered basin-wide. These intervals provide a comprehensive and
 363 reliable picture of climatological changes in the basin over the last several decades which can be

364 then applied to describe and attribute corresponding natural responses within the hydrological
365 system.

366 Five distinct climate intervals are identified since 1984, the most prominent of these is
367 termed the ‘Mega Drought’ which began in 2003 following a period of less extreme drought and
368 two very wet years. We identify this drought by consecutive years of annual precipitation deficits
369 of between 12% and 33% in basin-wide precipitation over almost a decade, paired with strong
370 decreases in precipitation across all stations after 2002. Due to the significance and region-wide
371 nature of this phenomenon, it was labeled a Mega Drought by a recent study (Garreaud et al.,
372 2020), and major deficits were also documented by researchers in northwestern Argentina during
373 this period (Ferrero et al., 2019). Following the Mega Drought, the climate regime at SdA has
374 become wetter but also significantly more variable, with several years of anomalously high
375 precipitation followed by years of anomalously low totals. This recent period is punctuated by
376 three of the largest widespread precipitation events in the instrumental record occurring in 2015,
377 2017, and 2019. From late January to early February 2019, every station in the basin recorded
378 greater than their mean annual total over less than 3 weeks. This event particularly in the
379 southern and eastern parts of the basin was the most significant precipitation event on record.
380 These large events have become notably more common over the last decade and have major
381 observable impacts on surface water bodies, wetland vegetation, and overall storage in the basin.

382 *Hydrological Changes*

383 Changes observed in the SdA hydrological system (i.e., surface waters, vegetation, and
384 streamflow) and basin-scale TWSA correlate well with the climate intervals described above;
385 however, there are important differences in timing and magnitude of response to rainfall and
386 drought. Overall, during the drought periods average Surface Water Extent (SWE), vegetation
387 extent, and TWSA are reduced and stable year-to-year, while during wet intervals and large
388 precipitation events corresponding increases occur (**Figure 3**). SWE changes in the basin follow
389 a seasonal cycle of larger winter extents, when potential evaporation is low, and reach yearly
390 lows in the summer (**Figure 3a**). This annual behavior is out-of-phase with precipitation,
391 predominantly between December and March, although it appears that after large events such as
392 in 2001, 2017, and 2019, SWE responded strongly and quickly and did not recede fully until the

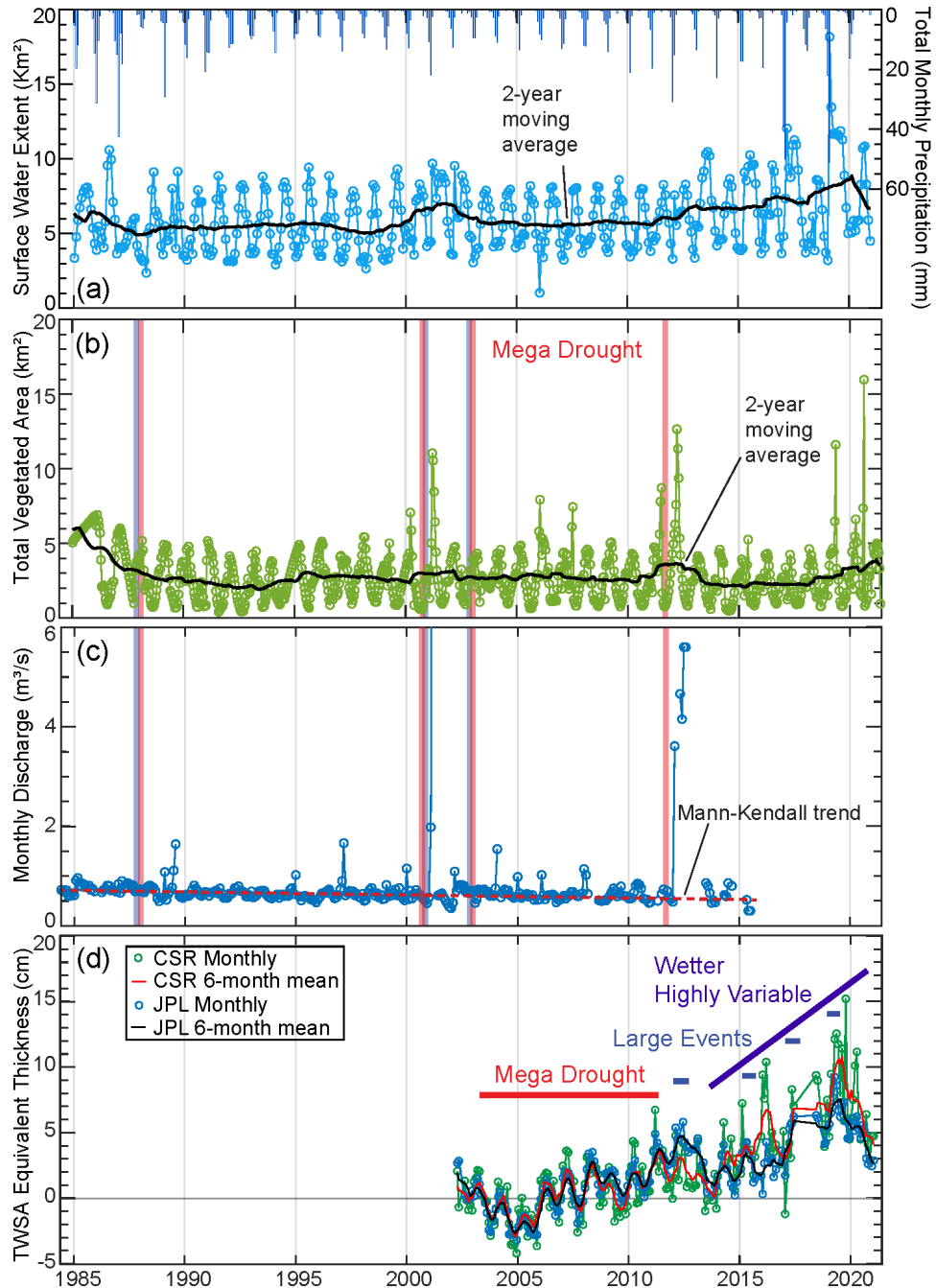


Figure 3. Changes in basin-wide hydrological conditions since 1985. **(a)** Total monthly surface water extent and TerraClimate total monthly precipitation, **(b)** total monthly extent of living vegetation, **(c)** average monthly discharge at the San Pedro stream gauge, and **(d)** GRACE-derived monthly terrestrial water storage anomaly equivalent thickness produced by JPL (green) and CSR (blue). Climate intervals are indicated with vertical bars and further detailed in **(d)** with the timing of large precipitation events.

393 following summer. Large increases in average SWE seen after 2012, which accelerated after
 394 2015 are primarily the result of these events adding large pulses of water to the system. During

395 the Mega Drought period, average extents are consistently low, similar to the drought in the
396 1990s, however, the winter maximums are consistently lower than that period. Vegetation
397 extents appear overall less variable than SWE, following an annual cycle in phase with summer
398 rainfall, and show a strong and rapid response to large rain events (**Figure 3b**). The period of
399 large events since 2015 has increased the total vegetation and SWE extent in the basin to the
400 highest levels since at least the 1980s.

401 Streamflow in the Rio San Pedro shows a clear response to large precipitation events,
402 particularly in 2001 (a maximum of 13 m³/s in March) and 2012 (**Figure 3c**). This strong
403 response likely reflects the efficient channeling of runoff in this large perennial river during these
404 events. These rapid responses are superimposed on a relatively small but consistent annual signal
405 of higher flows in the winter when evaporation is low and a consistent decreasing trend
406 throughout the record. A seasonal Mann-Kendall test of monthly average discharge in the river
407 recorded from 1984 to 2015 shows a statistically significant decreasing trend (p-value = 7.57E-
408 09) amounting to a total decrease in monthly streamflow of 0.01 m³/s. Changes in TWSA from
409 GRACE show a period of relatively low storage during the Mega Drought and a strong
410 increasing trend since then (**Figure 3d**). Since this drought also happens to coincide with the
411 baseline period over which the anomaly is determined, we cannot directly quantify the effect this
412 drought had on storage volumes relative to the period before. However, we can observe that
413 there was less total water stored in the basin during the drought than there was following the
414 large events in 2012 and especially during the wetter period that followed. Since the end of the
415 Mega Drought, terrestrial water storage in SdA has increased by a basin-wide equivalent
416 thickness of 3-10 cm. The clear annual signal in these data, like vegetation extent, is in phase
417 with summer precipitation and responds strongly and rapidly to large precipitation events while
418 also showing rapid declines during years with low rainfall. As Ahamed et al. (2021) show,
419 GRACE is quite effective at capturing responses to large recharge events. The similar response
420 in vegetation and water storage in the basin may reflect that these systems are primarily
421 responding to changes in shallow vadose zone soil moisture.

422 **4.2. Water Use and Lithium**

423 We present the first basin-wide assessment of allocated and actual freshwater use for
 424 SdA. **Figure 4a** shows the spatial distribution of water concessions scaled by permitted
 425 extraction allowances. We further differentiate and aggregate these data by water use type for
 426 both allocated (**Figure 4c**) and estimated actual use (**Figure 4d**). A review of the national
 427 database performed in cooperation with local parties yielded several observations about these
 428 allocations. Most of the water use permits are allocated to copper (“other mining”) and
 429 agriculture, which claim 47% and 34% of total water rights. The third and fourth highest
 430 allocations are lithium and potash mining companies with 10% and “other” uses with 7%.

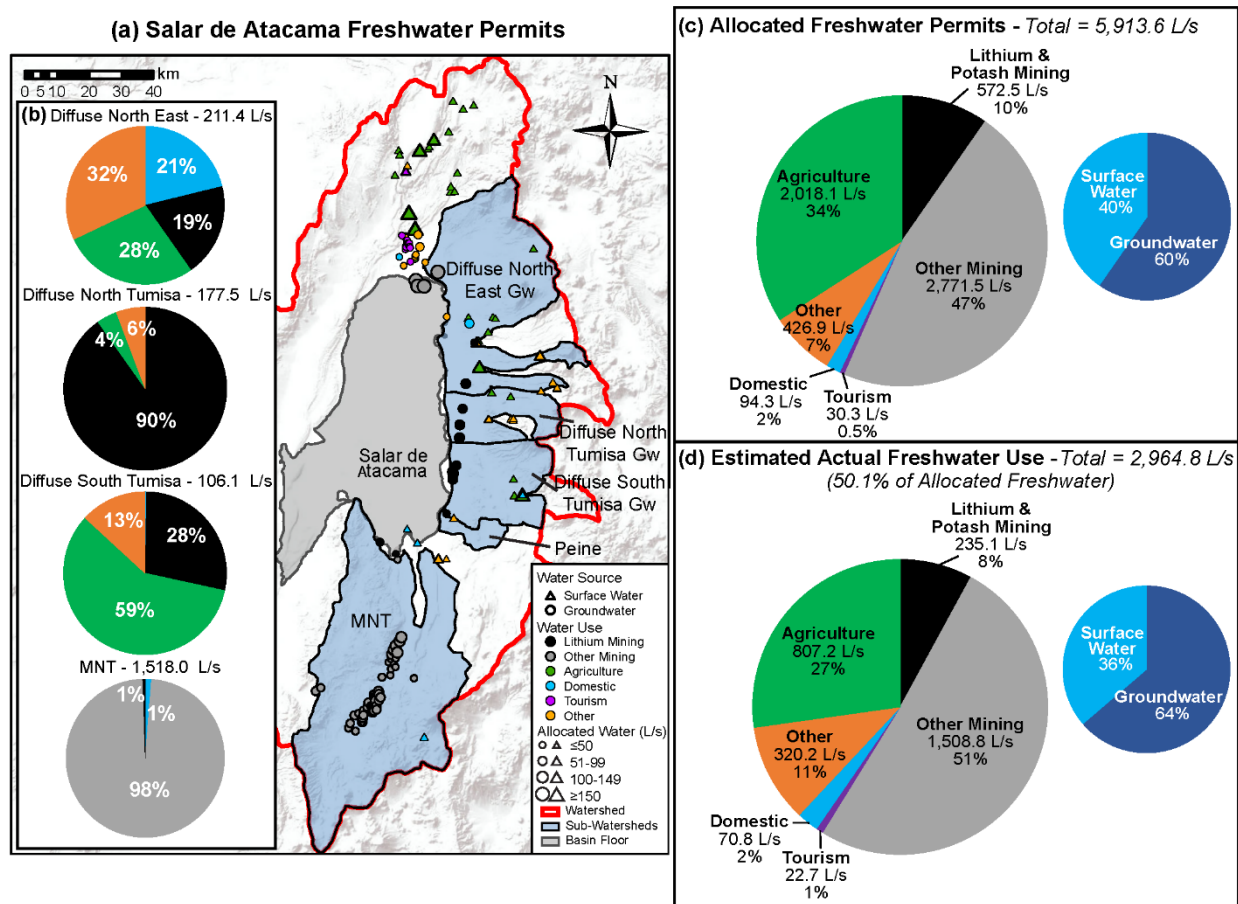


Figure 4. Freshwater allocation and use in the SdA basin. With (a) allocated freshwater permits divided by water source (symbol shape), use category (symbol color), and allocated amount (symbol size). (b) Pie charts of estimated actual freshwater use in 2014 within each sub-watershed zone divided by use category - lithium mining (black), other mining (grey), agriculture (green), domestic (blue), tourism (purple), and other (orange). No withdrawals occur within the Peine sub-watershed zone. Pie charts in (c) and (d) represent total allocated freshwater permits and estimated actual freshwater use in 2014, respectively.

431 Domestic uses make up 2% of total allocations, and water extraction that is strictly relevant to
432 the tourism industry comprises the remaining 0.5%.

433 Besides other mining extraction, agriculture is the second largest use type by category
434 and therefore we note the relative spatial disruption of agriculture versus mining in the basin.
435 First, most of the agricultural consumption is located upgradient of fresh groundwater extraction
436 for lithium and potash mining purposes (**Figure 4**). Second, agricultural freshwater consumption
437 consists primarily of surface water from streams located along the northern and eastern slopes of
438 the basin. Finally, it is important to note that the understanding of actual consumption is limited
439 to reported pumping rates from industrial users and poorly constrained estimates based on
440 hydrologic observations for non-industrial users. Therefore, there is substantial uncertainty in the
441 estimated freshwater use for agricultural purposes. Yet the estimates used in this study are
442 conservative considering the relative basin-wide impacts of agriculture on freshwater
443 consumption.

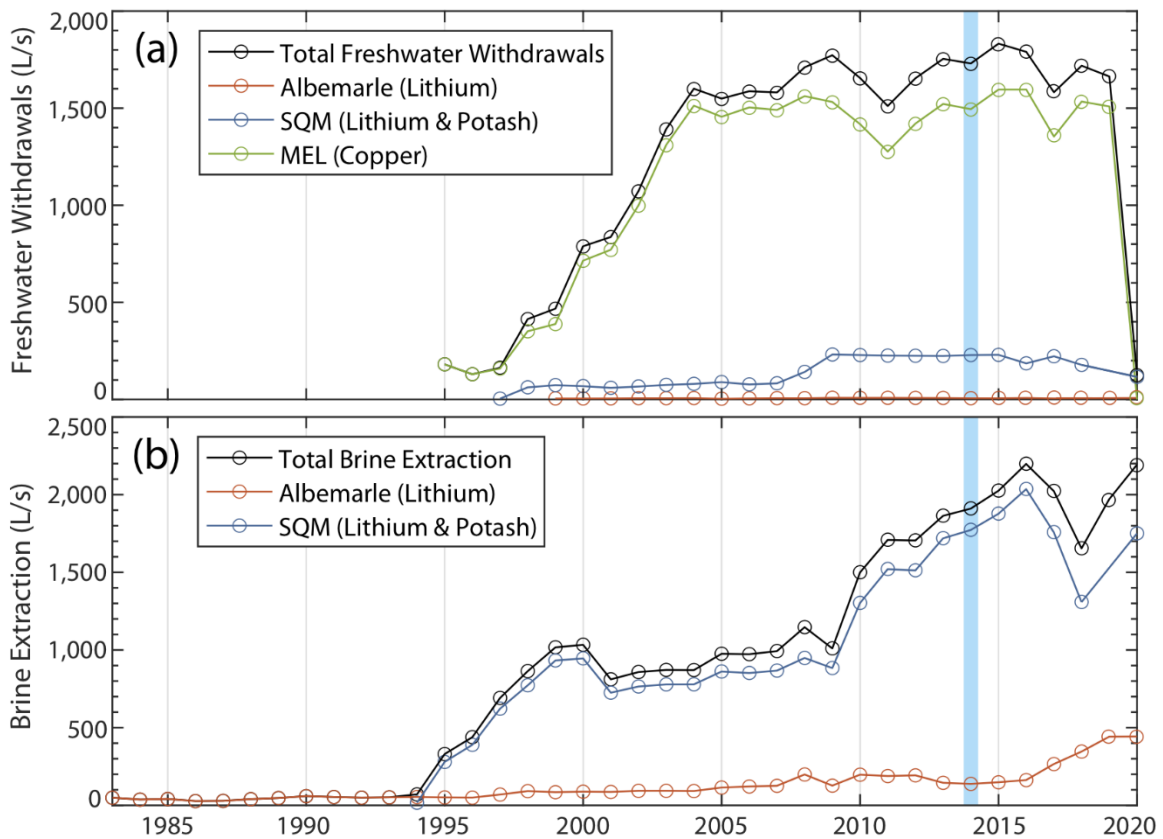


Figure 5. Annual freshwater (a) and brine (b) withdrawals associated with mining operations in the SdA basin. Minera Escondida Limitada extractions from ended in 2020. The blue bar represents the time frame (2014) of the water use assessment presented in **Figure 4d**.

444 Our findings illustrate that publicly available water extraction amounts do not equal
445 actual extraction in the basin. While several public reports have collated anthropogenic
446 extraction limits based on government-issued water use permits, we find that actual water use
447 has historically been monitored for industrial users and virtually unmonitored for private, non-
448 industrial users (AMPHOS21, 2018). **Figure 5** presents the history of both brine and freshwater
449 extraction within the basin. Freshwater extraction (**Figure 5a**) is separated by user to show the
450 relative contributions to total lithium and potash and other mining withdrawals in **Figure 4d**.
451 Specifically for lithium & potash mining, freshwater extraction is approximately 41% of
452 allocated water (i.e., 235.1 of 572.5 L/s), with Albemarle Corporation consuming 6.5 L/s and
453 SQM using 228.6 L/s in 2014 (blue bar in **Figure 5**). Thus, freshwater extraction for lithium
454 mining purposes equates to approximately 8% of total actual freshwater extraction for the basin.
455 Actual water use is further divided by sub-watershed zone to illustrate its spatial distribution and
456 potential impacts (**Figure 4b**). Most actual withdrawals (1,518.0 L/s) are from the MNT zone.
457 Diffuse North East, Diffuse North Tumisa, Diffuse South Tumisa, and Peine represent 211.4,
458 177.5, 106.1, and 0.0 L/s, respectively. A comparison between actual freshwater use in 2014 and
459 2020 are included in the supplemental material (**Figure S2**).

460 **4.3. Relic/Modern Water**

461 Inflows to the SdA hydrological system can be divided into three unique water
462 compartments or sources defined by their flow paths and mean transit times. This refined
463 understanding builds upon previous works by Jordan et al. (2002), Houston and Hart (2004),
464 Rissmann et al. (2015), Corenthal et al. (2016), Boutt et al. (2016), Moran et al. (2019), and
465 Munk et al. (2021). These sources are: i) direct precipitation and runoff (most of which does not
466 become groundwater recharge except perhaps within the salar nucleus) with short mean transit
467 times and residence in the system (weeks to months), most of this water leaves the basin as soil
468 or open water evaporation near the salar floor; ii) groundwater inflow from the large and deep
469 regional groundwater system which constitutes baseflow to springs and streams and the majority
470 of total inflow to the basin, these waters have long mean residence times ($\gg 65$ years) and are
471 largely decoupled from the influence of modern climate; and iii) local, intermediate
472 groundwaters with mean transit times on the order of 1-10 years, sourced predominantly from
473 local modern recharge within the high-infiltration capacity alluvial aquifers along the margin of

474 the basin floor. This third water source also likely contains large contributions of water from ^3H -
 475 dead stream water and springs and runoff from large rain events re-infiltrating along preferential
 476 pathways in the alluvium, therefore, its age distribution is likely highly spatially variable. We
 477 define the distribution of these three general water sources, their contributions to the

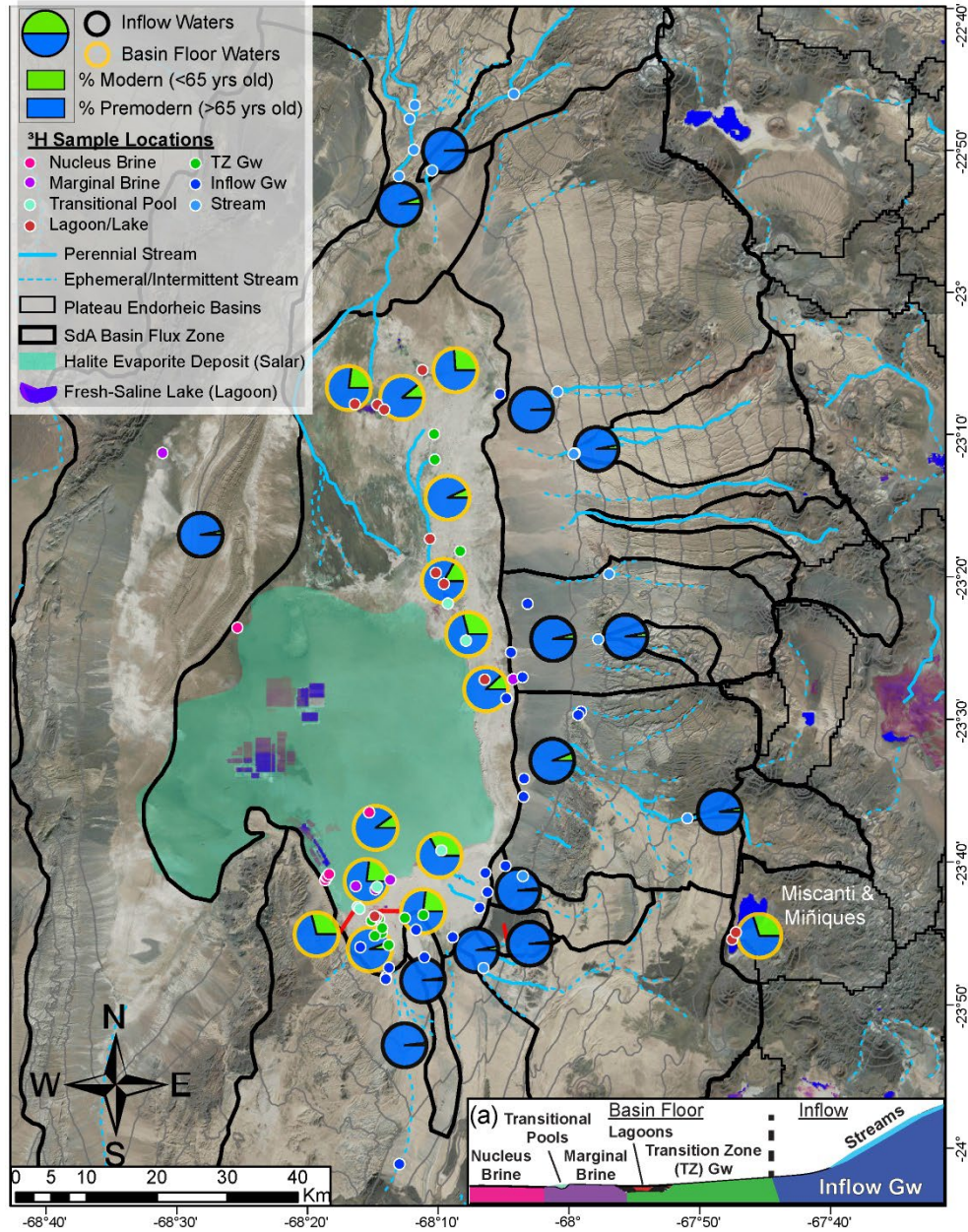


Figure 6. Distribution of modern/premodern (relic) water content. Pie charts show this ratio grouped by inflow zone (black outline) which includes springs, streams, and groundwaters, and basin floor water bodies (yellow outline). The high elevation lakes Miscanti & Miñiques outside the topographic watershed are included. Black lines delineate zones of flux into the basin and the approximate outline of the basin floor (as defined by Munk et al., 2018). Light grey lines are 250-meter contours of elevation. Colored dots show all samples collected for this work classified by water type (n=106). **(a)** Inset cross-sectional schematic defining the physical water body classifications.

478 hydrological budget, and their contributions to specific surface and groundwater bodies using ^3H
479 as a relative age tracer combined with other geochemical signatures.

480 We define the relative age of all surface and groundwater bodies within the SdA basin
481 using a large, comprehensive dataset collected over 10 years (**Figure 6**). Our results show
482 consistently low modern water content among inflow waters feeding the basin floor including all
483 streams, springs, and groundwater. Values range from 0% to 7% among 45 samples. One
484 additional sample is a notable outlier, containing 15% modern water, due to its location in an
485 alluvial fan near the salar margin at ~ 10 mbgl it may represent a local groundwater flow path
486 described above. By partitioning all basin inflows into sub-watersheds where the relative flux
487 was quantified by Munk et al. (2018) we show that most of the flux to the basin (57%) contains
488 very little modern water content ($\leq 4\%$), another 12% of flux contains an average of 6% modern
489 water but is skewed by the one outlier sample noted above. The final 31% of inflow to the basin
490 comes from the San Pedro River in the north with 5% modern water content. This river,
491 considering its large contribution to total inflow may act to transport small but focused amounts
492 of modern water to the basin floor. However, our results show that most of the inflow water
493 volume to the basin is composed of waters with essentially no modern content. Another
494 important result, which is apparent in **Figure 6** is the strong and consistent difference in modern
495 water content between the inflow waters and surface and groundwaters on the basin floor.

496 In contrast to the inflows, all water bodies on the basin floor (defined in **Figure 6a**)
497 contain a substantial proportion of modern water. The Transition Zone Groundwaters average
498 only 6% modern but range between 0% and 21% illustrating its position at the interface between
499 the basin inflows and the salar floor water bodies (the full statistical distribution of these water
500 bodies is shown in **Figure 7a**). In surface water bodies at the salar surface, the Lagoon waters
501 range between 8% and 28% and Transitional Pool waters between 16% and 53% indicating a
502 strong influence of modern inputs, strongest in the latter. As a point of reference, samples from a
503 pair of high elevation lakes near the watershed divide average about 30% modern, illustrating
504 that high modern water content in surface water bodies in this region is not unique to the SdA
505 basin floor. In the brine aquifers, the Marginal Brine contains between 2% and 36% modern, and
506 the Nucleus Brine contains between 2% and 20%. The presence of both ^3H -dead and high
507 modern content waters suggests that these brine aquifers receive inflow from multiple

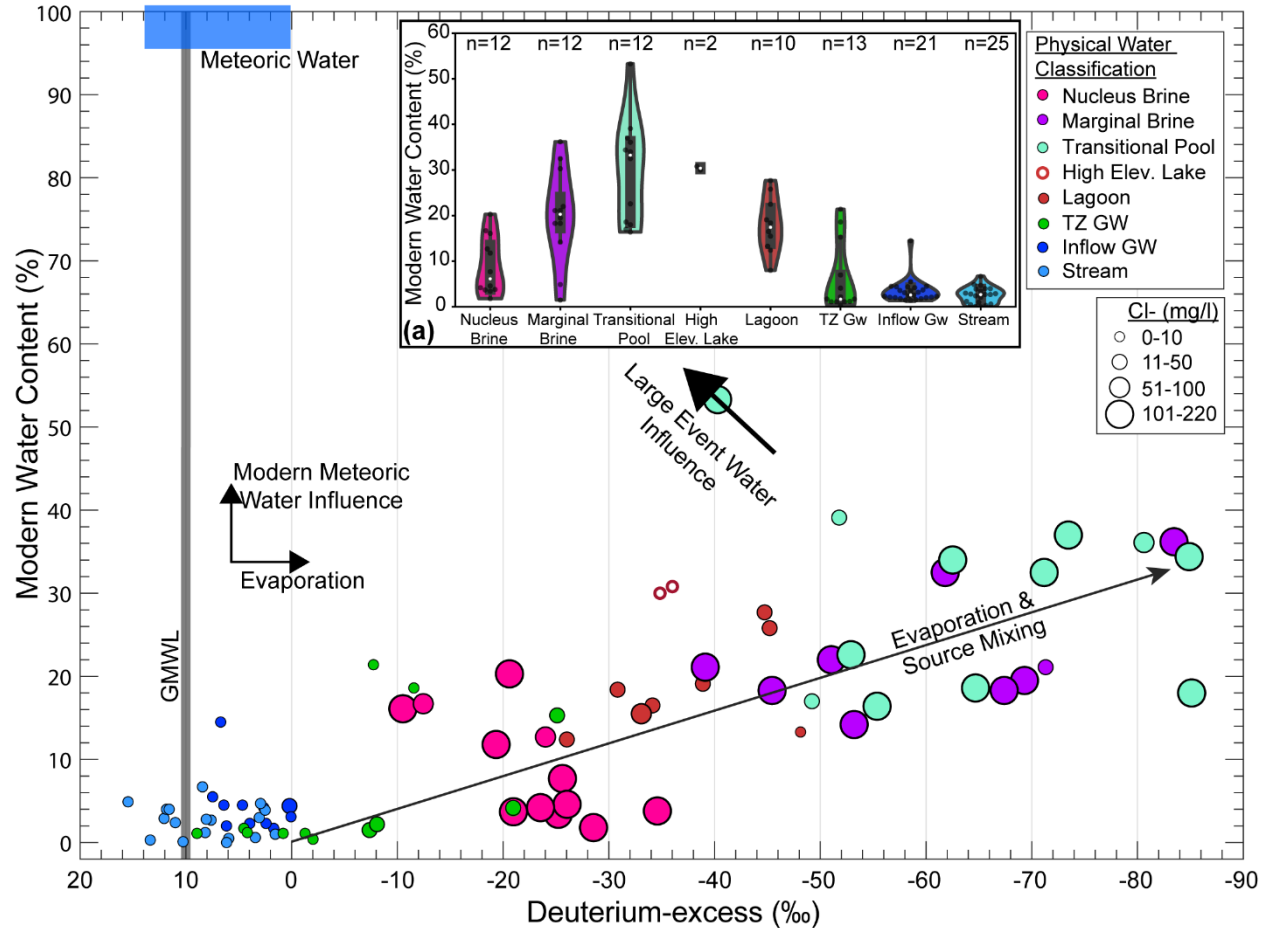


Figure 7. Processes controlling physical water distinctions and interactions. Circles are proportional to chloride concentration in each sample. The grey vertical bar is the Global Meteoric Water Line (GMWL), and the blue box represents the approximate range of meteoric input waters (based on Moran et al., 2019 data). Arrows depict the influence of important hydrological processes and interactions. **(a)** Violin plot of all data grouped by physical water type. Grey boxes show the interquartile range; white dots are the median and the colored polygons represent the frequency distribution of the data (black dots).

508 compartmentalized sources. The compartmentalization of water bodies and their interactions in
 509 the SdA system is illustrated in **Figure 7**.

510 The relationship between relative water age and deuterium-excess as well as Cl^-
 511 concentrations in sampled waters allows for the differentiation of distinct water bodies based on
 512 their dominant source and degree of interaction with the atmosphere. This interaction in this very
 513 arid environment imprints a strong evaporative signature on the stable H and O isotopes in water,
 514 resulting in increasing negative deuterium excess. Important results here include the strong
 515 differentiation of inflow waters from the brines and surface waters on the basin floor. This
 516 consistent signature suggests these inflow waters have been segregated from the atmosphere over

517 their entire transit, as there is no evidence of evaporation. These waters are sourced from relic
518 recharge, nearly all their volume is water that entered the ground at least 65 years ago. In
519 contrast to these waters, the surface water bodies and brines show both a strong signal of
520 evaporation and a higher proportion of modern water. The Transitional Pools have the highest
521 median percent modern value and the strongest evaporative signature (**Figure 7a**) likely
522 reflecting that their primary source is large modern rain events that flood the margin of the salar,
523 then rapidly evaporate and become saline. The Marginal Brines interestingly have a quite similar
524 signature to these surface waters suggesting a proportion of these waters share a similar source.
525 Brines contained within the nucleus aquifer are quite distinct from both the inflow and the
526 marginal brine and surface waters indicating inputs from several sources that may be somewhat
527 compartmentalized, some from mixtures containing mostly relic but evaporated water, and some
528 from a source containing more modern but less evaporated water. The Lagoon waters and
529 Transition Zone Gw results indicate they are likely sourced by a combination of relic inflow
530 water and modern rainwater. Lagoon waters contain high modern content and strong evaporation
531 signatures but are also fresher than the Brines and Transitional Pools. The shallow groundwaters
532 in the transition zone on the other hand are quite variable, some appear very similar to the old,
533 fresh inflow waters and some more similar to the Nucleus Brine and Lagoon waters. This likely
534 reflects the fact that they are at the interface between the regional inflow and basin floor, so they
535 are fed by inflow waters but also by modern meteoric waters that feed the surface waters near the
536 basin floor. These results again reiterate that the basin water budget is dominated by regional
537 inflow waters but also that critical insight can be gained by understanding the distinct sources in
538 the system.

539 The modern/premodern (relic) water ratios presented here are relative values based on the
540 estimated input activity of precipitation and surface and groundwater samples whose value
541 represents an unknown distribution of ages. Therefore, to better contextualize these values within
542 a physical framework we use a simple piston flow transit model to predict modern water content
543 at sample sites based on logical physical properties. This allows for a direct comparison between
544 our observations of water age from the field and those predicted within a strictly physical
545 framework. This model is highly conservative, intentionally reducing assumptions as much as
546 possible, and utilizes parameters from a simple model in a similar arid environment presented by
547 Houston (2007). We calculated the distance and gradient from the watershed divide directly

548 upgradient of 16 sampled inflow waters dispersed along the basin margin and applied a range of
 549 physical properties to estimate seepage velocities and transit times between the recharge area and
 550 sample site. Assuming recharge waters have a ^3H activity equal to that of modern meteoric
 551 water, we decayed that input over the transit time to the discharge point. As described above, we
 552 know that most of the inflow to the basin is groundwater so we (conservatively) assume that
 553 water emerging at the sample site will be a mixture of 2/3 this decayed recharge water and 1/3
 554 meteoric water that has been decayed one year to represent recent recharge infiltrating and
 555 mixing with these waters. The activity in this mixture is the model-predicted activity of water
 556 emerging from the ground at the sample site. Comparing the water composition predicted by this
 557 model using a range of plausible hydraulic conductivities and our measurements in the field, the
 558 physically-based model consistently predicts percent modern water content in inflow waters
 559 greater than an order of magnitude higher than we observe (**Figure 8**). Again, this model is
 560 highly conservative and not designed to directly model the flow of regional groundwater in the
 561 basin, but it serves to illustrate that the assumption of springs, groundwater, and streams, which
 562 are essentially ^3H -dead, as sourced from recharge entering and discharging the basin on modern

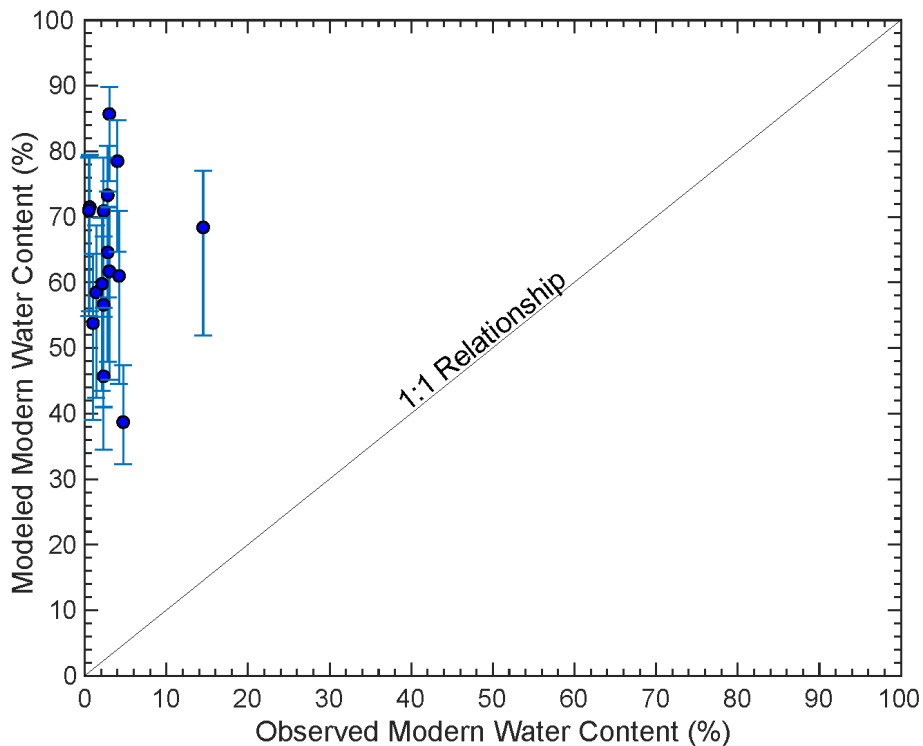


Figure 8. Modeled versus observed percent modern values at major sample sites with the line of direct 1:1 relationship. Modeled values are based on the piston flow transit model described in section 4.2. Blue dots are modeled values ($K = 10$ m/d), high-low range represented by $K=15.5$ m/d and $K= 5$ m/d respectively.

563 time scales cannot be reconciled with observations. The discrepancy between observed and
 564 modeled values also highlights that the existing conceptual models of this system, at modern
 565 hydrological balance are not capturing the fundamental hydrological dynamics required to
 566 adequately constrain the water budget. A complete description of the data and calculations for
 567 this model are presented in **Table S2**.

568 4.4. Water Budget with Relic Water

569 To illustrate the meaning of our findings we compare the existing conceptualization of
 570 the SdA water budget used by the DGA to manage water use in the basin (DGA, 2013) to a
 571 revised conceptualization that incorporates our understanding of water fluxes and sources (Boutt
 572 et al., 2021). These conceptualizations are summarized in a Sankey diagram (**Figure 9**) that

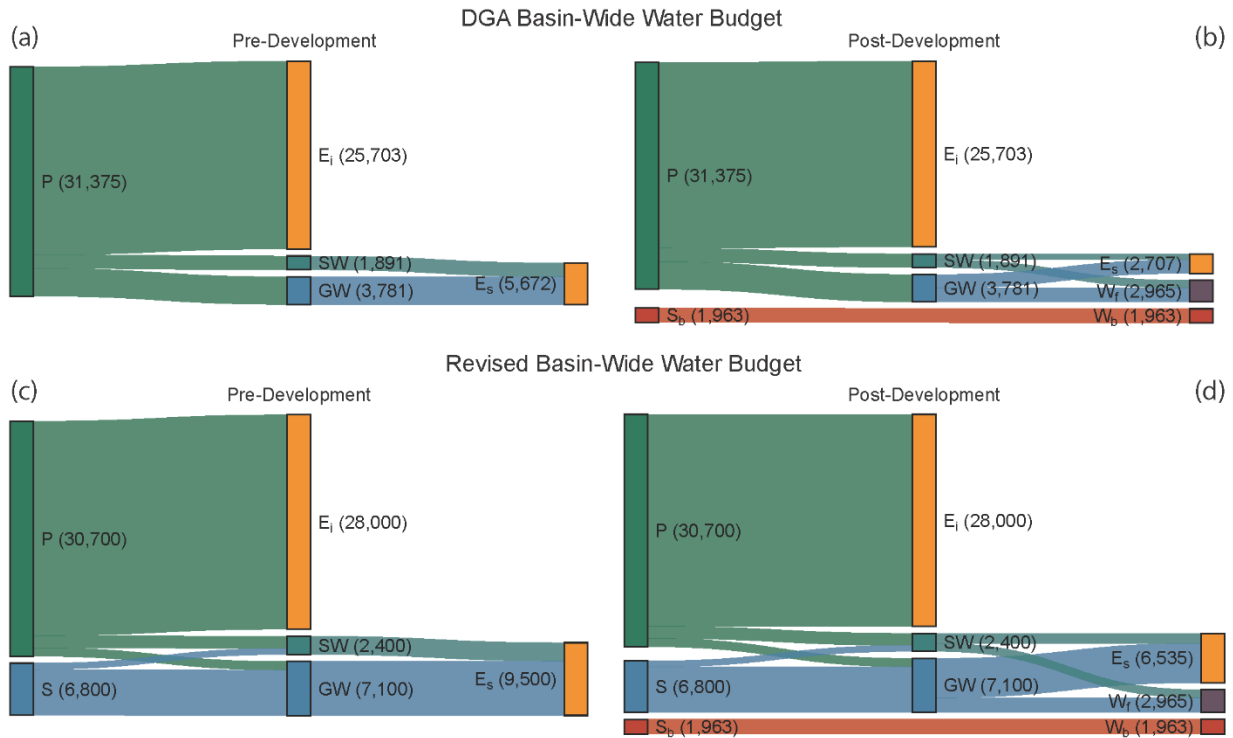


Figure 9. Current (DGA) and revised conceptualizations of the SdA basin water budget. Sources of water are on the left side of the Sankey diagrams and sinks are on the right. All terms represent water or brine flux in units of L/s. Precipitation (P) becomes infiltration losses due to evaporation (E_i) or the modern recharge component to surface water (SW) and groundwater (GW). **(a)** Current DGA conceptualization of the water budget without anthropogenic withdrawals with all SW and GW flux resulting in evaporation on or near the salar floor (E_s). **(b)** Current DGA conceptualization of the water budget with anthropogenic water withdrawals (W_f) and brine withdrawals (W_b) from storage in the brine body (S_b). **(c)** Revised conceptualization of the water budget with additional groundwater flux from storage (S). **(d)** Revised conceptualization of the water budget including anthropogenic withdrawals.

573 shows the pre-development understanding of the water budget (**Figure 9a,c**) and the impacts that
574 anthropogenic water use would have on the water budget (**Figure 9b,d**). Details of the data and
575 calculations are provided in the supplemental information (**Text S2**).

576 The DGA conceptualization (DGA, 2013) presented in **Figure 9a** assumes that the
577 system is at a steady-state within the topographic watershed. With this assumption, the modern
578 recharge, which is the sum of precipitation flux (P) to surface water (SW) and groundwater
579 (GW), balances all evapotranspiration from the salar (E_s) with no net storage flux (S). As
580 presented above, the assumption that all flux comes from modern recharge and flows along intra-
581 basin flow paths (<50 km) to the basin floor is not supported by our relative water age
582 observations. Also, based on this conceptualization, the net basin yield is 18% of P , a number
583 that is extremely large for arid watersheds even when accounting for infiltration from large and
584 infrequent precipitation events (Scanlon et al., 2006; Houston, 2009; Boutt et al., 2021).

585 We then apply anthropogenic freshwater (W_f) and brine (W_b) withdrawal estimates for
586 the basin to the DGA conceptualization of the water budget (**Figure 9b**), assuming that all W_b
587 flux results in a corresponding net storage flux from the brine body (S_b). We find that W_f results
588 in a 48% reduction in E_s to maintain the hydrologic balance within the steady-state assumption.
589 A portion of E_s includes the environmental flow requirement for sensitive wetland ecosystems
590 along the salar margin. Although the effects of a reduction in E_s on environmental flows are not
591 evaluated here, we assume that a reduction in E_s should result in some reduction in
592 environmental flows.

593 The revised conceptualization presented in **Figure 9c** does not assume steady-state
594 conditions within the topographic watershed and instead is based on flux estimate data from
595 1998 to 2009 (Boutt et al., 2021). The modern recharge estimate of 2,700 L/s (1,600 L/s to SW
596 and 1,100 L/s to GW) results in a net basin yield of 9%, which is significantly lower than the
597 DGA conceptualization. In this conceptualization, the majority (86%) of GW flux comes from S ,
598 which includes both pluvial groundwater storage within the basin from wetter past climate
599 regimes as well as long groundwater flow paths from outside of the topographic watershed
600 (Corenthal et al., 2016; Boutt et al., 2021), both of which are supported by our relative age
601 observations. **Figure 9d** applies the W_f and W_b estimates to the revised conceptualization with
602 the same assumptions applied to S_b and E_s . This results in a 31% reduction in E_s to maintain the
603 hydrologic balance.

604 The revised conceptualization shows that by overestimating modern recharge and net
605 basin yield, the DGA conceptualization underestimates groundwater storage losses and
606 overestimates the relative change in E_s . Moreover, reductions in precipitation due to recent
607 droughts will manifest differently depending on the conceptualization of the water budget. The
608 reduction in modern recharge due to decreased precipitation during the recent drought periods,
609 although not directly quantified here, would have a larger impact on SW and GW flux under the
610 DGA conceptualization compared to the revised conceptualization.

611 **5. Discussion**

612 **5.1. Importance of groundwater residence time and natural variations to ground-** 613 **truthing hydrological interpretations**

614 Although the SdA hydrological system is controlled by regional groundwater draining
615 from storage, disconnected from the modern climate, short-term climate variations (droughts and
616 large rain events) significantly impact surface water bodies and soil moisture in the basin. In
617 addition, major droughts reduced SWE and vegetation extent while at the same time mining-
618 related water extractions (from lithium and copper) dramatically increased. Wet intervals and
619 extreme precipitation events during this period also had strong and rapid effects on the wetlands
620 and surface water bodies in the basin. Despite ongoing brine and freshwater extractions, multiple
621 extreme rain events since 2015 have increased SWE and vegetation extents overall, and total
622 terrestrial water storage has also increased substantially (**Figure 3d**), likely due to large pulses of
623 recharge from these extreme rain events making their way through thick vadose zones above the
624 regional groundwater table. These results highlight the important role that climate variations
625 have on the water budget irrespective of anthropogenic influence. Any analysis of hydrological
626 impacts in arid regions such as this must disentangle these climate variations from anthropogenic
627 effects.

628 As global climate change becomes increasingly apparent, assessing impacts in SdA in the
629 context of these changes will become even more important. Indeed, a recent study found that
630 mean annual temperatures have already increased by $>0.5^\circ\text{C}$ over large parts of the dry Andes
631 since the 1980s (Frau et al., 2021). The most recent projections of climate change in this region
632 over the next several decades show that average temperatures will continue to increase (by $2\text{-}5^\circ\text{C}$

633 by 2100), the duration of seasonal snow and ice cover will decrease (by ~30 days by 2100), and
634 though projections for precipitation range anywhere from a slight decrease to a slight increase
635 overall, the timing of rain events is likely to change and the intensity increase (Pabón-Caicedo et
636 al., 2020; Bambach et al., 2021). Recent work shows the potential for increasing overall moisture
637 supply and large precipitation events in this region due to a southward shift in the South
638 American Monsoon and available moisture from the Amazon (Jordan et al., 2019;
639 Langenbrunner et al., 2019; Pascale et al., 2019). The most recent period of extreme events
640 (2015-present) may be a direct reflection of these climate changes, and therefore these events
641 may become more frequent. As we have outlined in this work, these extreme events have a major
642 impact on the surface water and wetland systems of SdA.

643 Though it may seem intuitive to attribute periods of decline in surface waters, wetland
644 vegetation, and groundwater levels at the margin of the salar to intensive, industrial-scale
645 extraction of lithium-rich brine and fresh groundwater in a very dry environment, the framework
646 we describe here shows how climate variability confounds this attribution. Correlation does not
647 equal causation, and for the reasons outlined in this work, great care must be taken when
648 attributing causes to specific impacts. For instance, the Rio San Pedro, which is isolated from
649 any potential impacts from the long legacy of water extraction for mining operations, shows a
650 steady and statistically significant decline in discharge since the 1980s (**Figure 3c**). The
651 watershed of this river is large and likely receives water from a combination of the three sources
652 of inflow outlined in section 4.3. Although ^3H results show that most of its flow originates from
653 relic groundwater, decreases in shorter-term inputs, due to accumulated precipitation deficits
654 from two long-term droughts may contribute to a decline in overall flow over decadal time
655 scales. In addition, it is difficult to quantify the impacts of water use changes at the many
656 agricultural plots in the watershed (**Figure 4a**), which may also contribute to the decrease in
657 discharge from the largest river in the basin.

658 Freshwater use for lithium and potash mining has had a small impact compared to copper
659 mining and other water uses. Groundwater storage declines have occurred throughout the basin
660 but are most pronounced in the MNT aquifer, where copper mining groundwater extractions are
661 concentrated, and in the Diffuse North East sub-watershed zone, where the primary water users
662 are other uses, agriculture, and domestic (**Figure S3** and **Figure 4a**). Of the fresh groundwater

663 zones where anthropogenic extraction occurs, the two sub-watershed zones where lithium and
664 potash mining extractions are the most concentrated (Diffuse North Tumisa and Diffuse South
665 Tumisa) experienced the smallest groundwater storage declines. Focusing water conservation
666 efforts on the water users in the MNT aquifer and the Diffuse North East sub-watershed zone
667 would have the greatest impact in minimizing harm from the overallocation of water rights in the
668 basin.

669 As we have described here, surface waters and vegetated wetlands are supported in large
670 part by baseflows into shallow water tables from regional groundwater discharge but are also
671 quite sensitive to changes in modern precipitation. Declines in regional groundwater inflow have
672 major and lasting impacts on these systems; however, these effects can be offset at least at the
673 basin scale by increases in precipitation related to natural climate variations. Impact assessments
674 on local wetlands must account for both processes.

675 **5.2. Allocation of water rights and implications of brine extraction under an inadequate** 676 **hydrological understanding**

677 Current water allocations in SdA are based on an inadequate hydrological representation
678 of the system and as a result, are substantially greater than what can be replenished on modern
679 time scales. Most water currently being used is not derived from modern rainfall, but relic
680 groundwater stored in local and regional aquifers; this water may be a “sustainable” source of
681 water, but specific thresholds for extraction of these old waters must be determined. What
682 constitutes sustainable extraction depends heavily on the location of extraction as freshwater
683 aquifer extractions have larger and more rapid wetland impact potential than brine aquifer
684 extractions. Responsible water allocation must incorporate this important fact. As outlined in this
685 study, current conceptualizations of the source and residence time of waters being extracted are
686 inadequate, and therefore truly sustainable water use metrics have likely never been met.

687 There are a few key implications of this misallocation of water in the basin. The
688 assumption underlying current water allowances is that water use is sustainable or renewable if
689 total withdrawals do not exceed inflows from modern recharge within the topographic watershed
690 and runoff minus evaporative losses. Most of the groundwater entering the basin is, in fact,
691 decoupled from modern recharge and therefore is not being replenished on human time scales.

692 Allocation of this groundwater under the assumption that it is immediately replenished is the
693 primary reason that water has been overallocated. The impacts of this inaccurate assumption are
694 likely localized to areas near actual extraction. For instance, the large amounts of water allocated
695 to copper miners in the upper part of the MNT aquifer would be entirely sustainable if the DGA
696 water budget conceptualization was correct. However, as we have shown here, the concentrated
697 use of this water over several decades has led to drawdowns in the aquifer significantly greater
698 than other aquifers in the basin (**Figure S3**), indicating that this water use is not sustainable. This
699 aquifer drawdown may impact wetlands fed by this water. Sustainable metrics must be
700 determined based on the source and residence time of the specific waters being extracted, not
701 basin-wide inflow estimates within a steady-state water budget.

702 Not all water extraction is equal in the basin as illustrated by the strongly discretized
703 compartments in **Figure 7**. The impacts from brine extraction cannot be equated to the impacts
704 from fresh groundwater extraction. As shown here and in previous works (e.g., Munk et al.,
705 2021), the brines being extracted for lithium are hosted in aquifers that are disconnected (on
706 human time scales) from surface water and wetland systems at the margin of the salar while
707 regional groundwater inflows provide critical baseflows that maintain these systems. In 2014,
708 lithium mining made up only ~8% of total freshwater extraction in the basin whereas copper
709 mining made up ~51%, these values are representative of the approximate average annual
710 extraction rate over the past decade. Though the copper mines have ceased freshwater
711 withdrawals as of 2020 (**Figure 5a**), due to long response times in these systems, the impact
712 from two decades of intensive extraction will likely continue for some time. Although the
713 lithium mines are located much closer to sensitive wetland systems, the actual impacts from their
714 water use are significantly less than that of copper mining, corresponding to relative extraction
715 volumes from the same inflow waters. Therefore, water allocations must be adjusted within this
716 revised conceptual understanding if they are to meet and maintain truly sustainable metrics while
717 preventing local impacts to surface and groundwaters.

718 **5.3. Problems associated with prior assessments of water storage and NDVI changes in**
719 **the basin**

720 The environmental impacts of lithium brine mining necessitate investigation, yet several
721 scientific publications that address the subject assume environmental impacts based on
722 conceptualizations that are both dissonant with the current understanding of the hydrological
723 dynamics of the basin and inconsistent with data-based observations. One example is Liu et al.
724 (2019), which attempts to directly correlate environmental degradation with areal mining growth
725 using several remote sensing products from JRC and MODIS. While using the NDVI product
726 from MODIS as a key metric in this study, the authors attribute the full range of NDVI (-1 to 1)
727 as directly proportional to green vegetation loss whereas published applications of NDVI apply
728 thresholds to specific ranges for vegetation identification and differentiation. The authors’
729 approach is neither justified in the manuscript nor proven in previous studies and is discordant
730 with our analysis using NDVI within previously defined ranges to identify areas of vegetation,
731 which indicates that vegetated area has increased through the past decade (**Figure 3b**). A further
732 confounding issue is the inclusion of the built evaporation ponds in their NDVI assessment,
733 water bodies result in negative values in the index and thus would bias NDVI towards more
734 negative numbers. Their conclusion of expanding degradation is increasingly implausible when
735 considering that it has no grounding in the basin’s hydrology; precipitation has increased over
736 recent years following the extreme drought and spring and surface water recharge is dominated
737 by relic water.

738 Another recent publication by Liu & Agusdinata (2020) argues that extraction of brine in
739 SdA over the last few decades has led directly to a decline in terrestrial water storage in the
740 basin, directly contradicting the results presented in this work (**Figure 3d**). Using GRACE
741 TWSA, they argue that between 2002 and 2017 water storage in the SdA basin declined at a rate
742 of 1.16 mm/year; however, the method presented to extract, process, analyze and interpret these
743 data is fundamentally flawed for several reasons. The source of data is a pre-processed GRACE
744 dataset hosted by the University of Colorado Boulder ([http://geoid.
745 colorado.edu/grace/index.html](http://geoid.colorado.edu/grace/index.html)), but the authors do not adequately describe the processing
746 performed to justify their results, making their results not reproducible. The domain over which
747 their analysis was conducted is not clearly defined, and the authors do not justify why the region

748 assessed is appropriate to reach their conclusions about SdA. The USGS Level 2 river basin
749 boundary (described as the domain of their analysis) encompasses an area much larger than the
750 SdA basin, including a large portion of the hyper-arid Atacama Desert and the Pacific coast,
751 >100km to the west of the SdA watershed. They assume that trends observed over this much
752 larger domain reflect changes in water storage in the SdA basin without providing supporting
753 evidence. The dataset used for their results utilizes a land surface-hydrological model (GLDAS-
754 CLM Hydrology) as a gain factor to scale the filtered GRACE data. However, an independent
755 assessment of this model within the SdA basin showed a strong increasing trend in storage,
756 opposite to that presented by the authors (**Figure S4**). As described in Landerer & Swenson
757 (2012), the gain factors derived from the model outputs used to scale the GRACE data are
758 intended to reduce small errors in the GRACE data from signal modification (e.g., attenuation).
759 In this case, the scaling has reversed the resulting trend, not merely reduced small errors. Even if
760 the negative trend they describe is to be believed, the magnitude of change is very small (1.16
761 mm/year) and given that the magnitude of storage changes observed by GRACE and that the
762 uncertainty associated with those data are at centimeter-scale, this trend could be within the
763 margin of error of the dataset. There is no explanation of whether this trend is statistically
764 significant and no assessment of error. In addition to SdA, our independent analysis of GLDAS
765 also found a positive trend in the Atacama region within their domain, leading us to conclude
766 that this major discrepancy likely results from known issues with using GRACE data and model
767 scaling factors for near-coastal regions (Wiese et al., 2016). These issues in addition to the fact
768 that an assessment of GRACE within the SdA basin by Montecino et al. (2016) and our analysis
769 of the SdA basin show a strong increase in total TWSA over the same period of ~5 cm (**Figure**
770 **3d**), illustrates serious flaws in the analysis by Liu and Agusdinata (2020). The lack of
771 confidence in the validity of these results discredits any conclusions reached therein about water
772 availability changes at SdA.

773 **5.4. Global implications of approach and results**

774 This work constitutes a comprehensive assessment of the SdA hydrological system
775 specifically; however, this work has both regional and global implications regarding the
776 assessment of water resource sustainability in drylands. First, the Mega Drought we've identified
777 at SdA is part of a continental-scale phenomenon that is one of the longest and most severe

778 droughts of the past millennium in this region (Morales et al., 2020, Garreaud et al., 2020). The
779 region hosts dozens of salar systems that display a similar set of climatic and hydrogeologic
780 conditions that manifest in similar fundamental hydrological controls (Moran, 2022). The
781 responses to anthropogenic and natural changes we document at SdA can therefore be directly
782 applied to understand these environmental impacts in basins across the region. This drought has
783 also been directly tied to the similarly anomalous Mega Drought currently occurring in the
784 western United States, both are likely triggered or greatly exacerbated by global climate change
785 (Steiger et al., 2021; Garreaud et al., 2021). The western US also contains many lithium-bearing
786 salars currently being explored for development, the water resources in these arid basins can also
787 benefit greatly from an improved understanding of these systems. The method we've applied to
788 document and interpret hydrological changes and responses in these environments addresses key
789 issues of water, human well-being, ecosystems, and climate in connection with global resource
790 and energy needs critical to our common future. Our findings make key advancements in our
791 understanding of natural water cycles in arid regions, current and future impacts from global
792 climate change, and new insights into the unique and elusive features of brine groundwater
793 hydrology.

794 **6. Conclusions**

795 Utilizing lithium brine and freshwater resources in arid basins while effectively
796 mitigating impacts from its extraction is unattainable without a comprehensive science-based
797 understanding of these hydrological and geochemical systems. Our approach is the most rigorous
798 and complete hydrological assessment of the SdA basin to date, outlining persistent
799 shortcomings in current water allocations and evaluation of impacts. We outline a method to
800 address these issues in the SdA basin that can be directly applied to the many arid endorheic
801 basins globally with significant current or future water demands. Our analysis shows that
802 climatological variations at SdA have caused major natural changes in surface water and
803 vegetation extent, streamflow, and basin-scale water storage on annual and decadal scales.
804 Anthropogenic water extraction has had important localized impacts on surface and
805 groundwaters, which are discussed here, but these changes can only be attributed after
806 accounting for the influence of natural variation. Relative extraction by different users must also
807 be considered when attributing impacts, especially with freshwater extraction which has a much

808 larger impact on wetlands, lagoons, and freshwater resources than brine extraction. The largest
809 freshwater users in the basin have been copper mining and agriculture, and the largest
810 groundwater storage losses have occurred where these two users are concentrated.

811 In addition, we show that the current SdA water budget is based on an outdated and
812 inadequate understanding of fundamental hydrological processes making it insufficient to
813 allocate water rights at sustainable extraction rates. We document that most of the current inflow
814 to the basin was recharged before the modern climate regime; therefore allocating water rights
815 based on an assumption of a system in steady-state with the modern climate is inherently flawed.
816 The considerable overallocation of water in the basin sub-catchments over the past few decades
817 has stemmed primarily from assumptions that overestimate water resource sustainability,
818 illustrated in our revised water budget. Future work on the water budget of SdA (and other arid
819 lithium-bearing basins) must recognize and explain the role of relic groundwater in the water
820 budget and explicitly incorporate geochemical tracer data into physical hydrologic models.
821 Furthermore, our new conceptual framework highlights the need to assess water extraction rates
822 in the context of sources of the water being extracted since responses to perturbations (natural or
823 anthropogenic) can be very different depending on where extraction is occurring (i.e., brine
824 aquifers vs fresh marginal aquifers). This work has far-reaching implications for future water
825 management and mitigation of impacts in the SdA basin and is an effective guide to sustainably
826 utilize water and brine resources globally.

827 **Acknowledgments**

828 The authors would like to thank BMW Group and BASF SE for funding and supporting
829 this research. We also want to thank Ricki Sheldon and the Council of Peoples Atacameños for
830 graciously volunteering to conduct a sampling campaign that was pivotal to this study. In
831 addition, we would like to thank Dr. Matt Winnick and Dr. Justin Richardson for access to their
832 analytical geochemistry instruments and equipment, and Alex Grant for valuable perspective and
833 feedback on this manuscript. There are no real or perceived financial conflicts of interest for any
834 of the authors.

835 **Open Research**

836 Raw data used to produce the remote sensing results presented in section 4.1, and all data
837 included in the supplementary information are compiled in an open access data repository for
838 this work (<https://doi.org/10.7275/e7t9-ta95>).

839 **Figure Captions:**

840 **Figure 1.** Major lithium-bearing basins of the Dry Andean Plateau of South America. (a) The
841 regional mean annual precipitation of the region and the SdA basin topographic watershed are
842 outlined in red. (b) Inset map of the SdA basin and its hydrological features. The salar nucleus,
843 transition zone, surface waters, vegetated wetlands, and perennial streams are outlined.
844 Meteorological stations and the stream gauge are labeled along with the location of fresh
845 groundwater extraction wells. The MNT aquifer is highlighted in green, and streams (rivers) are
846 in blue.

847
848 **Figure 2.** Annual precipitation from 1984-2020. Vertical red/blue bars represent major climate
849 intervals identified. (a) Shows records from meteorological stations within the basin, the Rio
850 Grande station record is a dotted line due to its location at the northern end of the basin. (b) The
851 basin-wide area-integrated annual precipitation from the TerraClimate dataset with the 3-year
852 moving average. The Mean Annual Precipitation (MAP) from the TerraClimate record (1958-
853 present) is indicated by the blue horizontal line.

854 **Figure 3.** Changes in basin-wide hydrological conditions since 1985. (a) Total monthly surface
855 water extent and TerraClimate total monthly precipitation, (b) total monthly extent of living
856 vegetation, (c) average monthly discharge at the San Pedro stream gauge, and (d) GRACE-
857 derived monthly terrestrial water storage anomaly equivalent thickness produced by JPL (green)
858 and CSR (blue). Climate intervals are indicated with vertical bars and further detailed in (d) with
859 the timing of large precipitation events.

860 **Figure 4.** Freshwater allocation and use in the SdA basin. With (a) allocated freshwater permits
861 divided by water source (symbol shape), use category (symbol color), and allocated amount
862 (symbol size). (b) Pie charts of estimated actual freshwater use in 2014 within each sub-
863 watershed zone divided by use category - lithium mining (black), other mining (grey),
864 agriculture (green), domestic (blue), tourism (purple), and other (orange). No withdrawals occur
865 within the Peine sub-watershed zone. Pie charts in (c) and (d) represent total allocated freshwater
866 permits and estimated actual freshwater use in 2014, respectively.

867 **Figure 5.** Annual freshwater and brine withdrawals associated with mining operations in the
868 SdA basin. Minera Escondida Limitada extractions from ended in 2020. The blue bar represents
869 the time frame (2014) of the water use assessment presented in **Figure 4d**.

870
871 **Figure 6.** Distribution of modern/premodern (relic) water content. Pie charts show this ratio
872 grouped by inflow zone (black outline) which includes springs, streams, and groundwaters, and
873 basin floor water bodies (yellow outline). The high elevation lakes Miscanti & Miñiques outside
874 the topographic watershed are included. Black lines delineate zones of flux into the basin and the

875 approximate outline of the basin floor (as defined by Munk et al., 2018). Light grey lines are
876 250-meter contours of elevation. Colored dots show all samples collected for this work classified
877 by water type (n=106). (a) Inset cross-sectional schematic defining the physical water body
878 classifications.

879
880 **Figure 7.** Processes controlling physical water distinctions and interactions. Circles are
881 proportional to chloride concentration in each sample. The grey vertical bar is the Global
882 Meteoric Water Line (GMWL), and the blue box represents the approximate range of meteoric
883 input waters (based on Moran et al., 2019 data). Arrows depict the influence of important
884 hydrological processes and interactions. (a) Violin plot of all data grouped by physical water
885 type. Grey boxes show the interquartile range; white dots are the median and the colored
886 polygons represent the frequency distribution of the data (black dots).

887 **Figure 8.** Modeled versus observed percent modern values at major sample sites with the line of
888 direct 1:1 relationship. Modeled values are based on the piston flow transit model described in
889 section 4.2. Blue dots are modeled values ($K = 10$ m/d), high-low range represented by $K=15.5$
890 m/d and $K= 5$ m/d respectively.

891
892 **Figure 9.** Current (DGA) and revised conceptualizations of the SdA basin water budget. Sources
893 of water are on the left side of the Sankey diagrams and sinks are on the right. All terms
894 represent water or brine flux in units of L/s. Precipitation (P) becomes infiltration losses due to
895 evaporation (E_i) or the modern recharge component to surface water (SW) and groundwater
896 (GW). (a) Current DGA conceptualization of the water budget without anthropogenic
897 withdrawals with all SW and GW flux resulting in evaporation on or near the salar floor (E_s). (b)
898 Current DGA conceptualization of the water budget with anthropogenic water withdrawals (W_f)
899 and brine withdrawals (W_b) from storage in the brine body (S_b). (c) Revised conceptualization of
900 the water budget with additional groundwater flux from storage (S). (d) Revised
901 conceptualization of the water budget including anthropogenic withdrawals.

902
903

904 **References**

- 905 AghaKouchak, A., Mirchi, A., Madani, K., Di Baldassarre, G., Nazemi, A., Alborzi, A., ...
906 Wanders, N. (2021). Anthropogenic Drought: Definition, Challenges, and Opportunities.
907 *Reviews of Geophysics*, 59(2), 1–23. <https://doi.org/10.1029/2019RG000683>
- 908 Ahamed, A., Knight, R., Alam, S., Pauloo, R., & Melton, F. (2021). Assessing the utility of
909 remote sensing data to accurately estimate changes in groundwater storage. *Science of*
910 *The Total Environment*, 807, 150635. <https://doi.org/10.1016/j.scitotenv.2021.150635>
- 911 AMPHOS21 (2018). Estudio de modelos hidrogeológicos conceptuales integrados, para los
912 salares de Atacama, Maricunga y Pedernales. Comité de Minería No Metálica CORFO,
913 368.
- 914 Ambrose, H., & Kendall, A. (2020). Understanding the future of lithium: Part 1, resource model.
915 *Journal of Industrial Ecology*, 24(1), 80–89. <https://doi.org/10.1111/jiec.12949>
- 916 Anderson, M., Low, R., & Foot, S. (2002). Sustainable groundwater development in arid, high
917 Andean basins. *Geological Society, London, Special Publications*, 193(1), 133–144.
918 <https://doi.org/10.1144/GSL.SP.2002.193.01.11>
- 919 Ashraf, S., Nazemi, A., & AghaKouchak, A. (2021). Anthropogenic drought dominates
920 groundwater depletion in Iran. *Scientific Reports*, 11(1), 9135.
921 <https://doi.org/10.1038/s41598-021-88522-y>
- 922 Babidge, S., Kalazich, F., Prieto, M., & Yager, K. (2019). “That’s the problem with that lake; it
923 changes sides”: mapping extraction and ecological exhaustion in the Atacama. *Journal of*
924 *Political Ecology*, 26(1), 738–760. <https://doi.org/10.2458/v26i1.23169>
- 925 Bambach, N. E., Rhoades, A. M., Hatchett, B. J., Jones, A. D., Ullrich, P. A., & Zarzycki, C. M.
926 (2021). Projecting climate change in South America using variable-resolution
927 Community Earth System Model: An application to Chile. *International Journal of*
928 *Climatology*, (August), 1–29. <https://doi.org/10.1002/joc.7379>
- 929 Beria, H., Larsen, J. R., Ceperley, N. C., Michelon, A., Vennemann, T., & Schaefli, B. (2018).
930 Understanding snow hydrological processes through the lens of stable water isotopes.
931 *Wiley Interdisciplinary Reviews: Water*, (June), e1311.
932 <https://doi.org/10.1002/wat2.1311>
- 933 Bierkens, M. F. P., & Wada, Y. (2019). Non-renewable groundwater use and groundwater
934 depletion: a review. *Environmental Research Letters*, 14(6), 063002.
935 <https://doi.org/10.1088/1748-9326/ab1a5f>
- 936 Birkel, C., & Soulsby, C. (2015). Advancing tracer-aided rainfall-runoff modelling: a review of
937 progress, problems and unrealised potential. *Hydrological Processes*, 29(25), 5227–5240.
938 <https://doi.org/10.1002/hyp.10594>
- 939 Blard, P.-H., Sylvestre, F., Tripathi, A. K., Claude, C., Causse, C., Coudrain, A., ... Lavé, J.
940 (2011). Lake highstands on the Altiplano (Tropical Andes) contemporaneous with
941 Heinrich 1 and the Younger Dryas: new insights from 14C, U–Th dating and $\delta^{18}O$ of

- 942 carbonates. *Quaternary Science Reviews*, 30(27–28), 3973–3989.
 943 <https://doi.org/10.1016/j.quascirev.2011.11.001>
- 944 Bobst, A. L., Lowenstein, T. K., Jordan, T. E., Godfrey, L. V., Ku, T. L., & Luo, S. (2001). A 106
 945 ka paleoclimate record from drill core of the Salar de Atacama, northern Chile.
 946 *Palaeogeography, Palaeoclimatology, Palaeoecology*, 173(1–2), 21–42.
 947 [https://doi.org/10.1016/S0031-0182\(01\)00308-X](https://doi.org/10.1016/S0031-0182(01)00308-X)
- 948 Boulay, A.-M., Bare, J., Benini, L., Berger, M., Lathuillière, M. J., Manzardo, A., ... Pfister, S.
 949 (2018). The WULCA consensus characterization model for water scarcity footprints:
 950 assessing impacts of water consumption based on available water remaining (AWARE).
 951 *The International Journal of Life Cycle Assessment*, 23(2), 368–378.
 952 <https://doi.org/10.1007/s11367-017-1333-8>
- 953 Boutt, D. F., Hynek, S. A., Munk, L. A., & Corenthal, L. G. (2016). Rapid recharge of fresh
 954 water to the halite-hosted brine aquifer of Salar de Atacama, Chile. *Hydrological
 955 Processes*, 30(25), 4720–4740. <https://doi.org/10.1002/hyp.10994>
- 956 Boutt, D.F., Corenthal, L.G., Moran, B.J. et al. Imbalance in the modern hydrologic budget of
 957 topographic catchments along the western slope of the Andes (21–25°S): implications for
 958 groundwater recharge assessment. *Hydrogeol J* 29, 985–1007 (2021).
 959 <https://doi.org/10.1007/s10040-021-02309-z>
- 960 Bredehoeft, J. D. (2002). The water budget myth revisited: Why hydrogeologists model. *Ground
 961 Water*, Vol. 40, pp. 340–345. <https://doi.org/10.1111/j.1745-6584.2002.tb02511.x>
- 962 Buttle, J.M. (1994). Isotope hydrograph separations and rapid delivery of pre-event water from
 963 basins drainage. *Phys. Geogr.* 18, 16–41.
- 964 Cabello, J. (2021). Lithium brine production, reserves, resources and exploration in Chile: An
 965 updated review. *Ore Geology Reviews*, 128(2020), 103883.
 966 <https://doi.org/10.1016/j.oregeorev.2020.103883>
- 967 Cartwright, I., Cendón, D., Currell, M., & Meredith, K. (2017). A review of radioactive isotopes
 968 and other residence time tracers in understanding groundwater recharge: Possibilities,
 969 challenges, and limitations. *Journal of Hydrology*, 555, 797–811.
 970 <https://doi.org/10.1016/j.jhydrol.2017.10.053>
- 971 Clark, I. & Fritz, P. (1997). *Environmental Isotopes in Hydrogeology*. Lewis Publications, Boca
 972 Raton, FL.
- 973 Cook, P.G. and Bohlke, J.K. (2000). Determining timescales for groundwater flow and solute
 974 transport. In: Cook, P.G., Herczeg, A.L. (Eds.), *Environmental Tracers in Subsurface
 975 Hydrology*. Kluwer, Boston, pp. 1–30.
- 976 Cordero, R. R., Asencio, V., Feron, S., Damiani, A., Llanillo, P. J., Sepulveda, E., ... Casassa, G.
 977 (2019). Dry-Season Snow Cover Losses in the Andes (18°–40°S) driven by Changes in
 978 Large-Scale Climate Modes. *Scientific Reports*, 9(1), 16945.
 979 <https://doi.org/10.1038/s41598-019-53486-7>
- 980 Corenthal, L. G., Boutt, D. F., Hynek, S. A., & Munk, L. A. (2016). Regional groundwater flow
 981 and accumulation of a massive evaporite deposit at the margin of the Chilean Altiplano.

- 982 Geophysical Research Letters, 43(15), 8017–8025.
 983 <https://doi.org/10.1002/2016GL070076>
- 984 Cortecchi, G., Boschetti, T., Mussi, M., Lameli, C. H., Mucchino, C., & Barbieri, M. (2005). New
 985 chemical and original isotopic data on waters from El Tatio geothermal field, northern
 986 Chile. *Geochemical Journal*, 39(6), 547–571. <https://doi.org/10.2343/geochemj.39.547>
- 987 DGA (Dirección General de Aguas) (2013). *Análisis de la Oferta Hídrica del Salar de Atacama*.
 988 Santiago, Chile.
- 989 Fan, Y., Li, H., & Miguez-Macho, G. (2013). Global Patterns of Groundwater Table Depth.
 990 *Science*, 339(6122), 940–943. <https://doi.org/10.1126/science.1229881>
- 991 Ferrero, M. E., & Villalba, R. (2019). Interannual and Long-Term Precipitation Variability
 992 Along the Subtropical Mountains and Adjacent Chaco (22–29° S) in Argentina. *Frontiers*
 993 *in Earth Science*, 7(July). <https://doi.org/10.3389/feart.2019.00148>
- 994 Frau, D., Moran, B. J., Arengo, F., Marconi, P., Battauz, Y., Mora, C., ... Boutt, D. F. (2021).
 995 Hydroclimatological Patterns and Limnological Characteristics of Unique Wetland
 996 Systems on the Argentine High Andean Plateau. *Hydrology*, 8(4), 164.
 997 <https://doi.org/10.3390/hydrology8040164>
- 998 Gajardo, G., & Redón, S. (2019). Andean hypersaline lakes in the Atacama Desert, northern
 999 Chile: Between lithium exploitation and unique biodiversity conservation. *Conservation*
 1000 *Science and Practice*, 1(9), 1–8. <https://doi.org/10.1111/csp2.94>
- 1001 Garreaud, R., Vuille, M., & Clement, A. C. (2003). The climate of the Altiplano: Observed
 1002 current conditions and mechanisms of past changes. *Palaeogeography,*
 1003 *Palaeoclimatology, Palaeoecology*, 194(1–3), 5–22. [https://doi.org/10.1016/S0031-](https://doi.org/10.1016/S0031-0182(03)00269-4)
 1004 [0182\(03\)00269-4](https://doi.org/10.1016/S0031-0182(03)00269-4)
- 1005 Garreaud, R. D., Boisier, J. P., Rondanelli, R., Montecinos, A., Sepúlveda, H. H., & Veloso-
 1006 Aguila, D. (2020). The Central Chile Mega Drought (2010–2018): A climate dynamics
 1007 perspective. *International Journal of Climatology*, 40(1), 421–439.
 1008 <https://doi.org/10.1002/joc.6219>
- 1009 Garreaud, R. D., Clem, K., & Veloso, J. V. (2021). The South Pacific Pressure Trend Dipole and
 1010 the Southern Blob. *Journal of Climate*, 34(18), 7661–7676. [https://doi.org/10.1175/JCLI-](https://doi.org/10.1175/JCLI-D-20-0886.1)
 1011 [D-20-0886.1](https://doi.org/10.1175/JCLI-D-20-0886.1)
- 1012 Gayo, E. M., Latorre, C., Jordan, T. E., Nester, P. L., Estay, S. A., Ojeda, K. F., & Santoro, C.
 1013 M. (2012). Late Quaternary hydrological and ecological changes in the hyperarid core of
 1014 the northern Atacama Desert (~21°S). *Earth-Science Reviews*, 113(3–4), 120–140.
 1015 <https://doi.org/10.1016/j.earscirev.2012.04.003>
- 1016 Gleeson, T., Marklund, L., Smith, L., & Manning, A. H. (2011). Classifying the water table at
 1017 regional to continental scales. *Geophysical Research Letters*, 38(5), n/a-n/a.
 1018 <https://doi.org/10.1029/2010GL046427>
- 1019 Godfrey, L., Jordan, T., Lowenstein, T., & Alonso, R. (2003). Stable isotope constraints on the
 1020 transport of water to the Andes between 22° and 26°S during the last glacial cycle.

- 1021 Palaeogeography, Palaeoclimatology, Palaeoecology, 194(1–3), 299–317.
 1022 [https://doi.org/10.1016/S0031-0182\(03\)00283-9](https://doi.org/10.1016/S0031-0182(03)00283-9)
- 1023 Grosjean, Martin; Geyh, Mebus A.; Messerli, Bruno; Schotterer, U. (1995). Late-glacial and
 1024 early Holocene lake sediments, groundwater formation and climate in the Atacama
 1025 Altiplano 22-24°S. *Journal of Paleolimnology*, 14, 241–252.
- 1026 Grosjean, M., & Núñez, A. L. (1994). Lateglacial, early and middle holocene environments,
 1027 human occupation, and resource use in the Atacama (Northern Chile). *Geoarchaeology*,
 1028 9(4), 271–286. <https://doi.org/10.1002/gea.3340090402>
- 1029 Gutiérrez, J. S., Navedo, J. G., & Soriano-Redondo, A. (2018). Chilean Atacama site imperilled
 1030 by lithium mining. *Nature*, 557(7706), 492–492. <https://doi.org/10.1038/d41586-018-05233-7>
- 1032 Herrera, C., Custodio, E., Chong, G., Lambán, L. J., Riquelme, R., Wilke, H., ... Lictevoud, E.
 1033 (2016). Groundwater flow in a closed basin with a saline shallow lake in a volcanic area:
 1034 Laguna Tuyajto, northern Chilean Altiplano of the Andes. *Science of The Total*
 1035 *Environment*, 541, 303–318. <https://doi.org/10.1016/j.scitotenv.2015.09.060>
- 1036 Houston, J. (2002). Groundwater recharge through an alluvial fan in the Atacama Desert,
 1037 northern Chile: mechanisms, magnitudes and causes. *Hydrological Processes*, 16(15),
 1038 3019–3035. <https://doi.org/10.1002/hyp.1086>
- 1039 Houston, J. (2006). Variability of precipitation in the Atacama Desert: Its causes and
 1040 hydrological impact. *International Journal of Climatology*, 26(July), 2181–2198.
 1041 <https://doi.org/10.1002/joc>
- 1042 Houston, J. (2007). Recharge to groundwater in the Turi Basin, northern Chile: An evaluation
 1043 based on tritium and chloride mass balance techniques. *Journal of Hydrology*, 334(3–4),
 1044 534–544. <https://doi.org/10.1016/j.jhydrol.2006.10.030>
- 1045 Houston, J. (2009). A recharge model for high altitude, arid, Andean aquifers. *Hydrological*
 1046 *Processes*, 23(16), 2383–2393. <https://doi.org/10.1002/hyp.7350>
- 1047 Houston, J., & Hart, D. (2004). Theoretical head decay in closed basin aquifers: an insight into
 1048 fossil groundwater and recharge events in the Andes of northern Chile. *Quarterly Journal*
 1049 *of Engineering Geology and Hydrogeology*, 37(2), 131–139.
 1050 <https://doi.org/10.1144/1470-9236/04-007>
- 1051 Jasechko, S. (2016). Partitioning young and old groundwater with geochemical tracers. *Chemical*
 1052 *Geology*, 427, 35–42. <https://doi.org/10.1016/j.chemgeo.2016.02.012>
- 1053 Jones, D. B., Harrison, S., Anderson, K., & Whalley, W. B. (2019). Rock glaciers and mountain
 1054 hydrology: A review. *Earth-Science Reviews*, 193, 66–90.
 1055 <https://doi.org/10.1016/j.earscirev.2019.04.001>
- 1056 Jordan, T. E., Munoz, N., Hein, M., Lowenstein, T., Godfrey, L., & Yu, J. (2002). Active
 1057 faulting and folding without topographic expression in an evaporite basin, Chile. *Bulletin*
 1058 *of the Geological Society of America*, 114(11), 1406–1421. [https://doi.org/10.1130/0016-7606\(2002\)114<1406:AFAFWT>2.0.CO;2](https://doi.org/10.1130/0016-7606(2002)114<1406:AFAFWT>2.0.CO;2)

- 1060 Jordan, T. E., Herrera L., C., Godfrey, L. V., Colucci, S. J., Gamboa P., C., Urrutia M., J., ...
 1061 Paul, J. F. (2019). Isotopic characteristics and paleoclimate implications of the extreme
 1062 precipitation event of March 2015 in northern Chile. *Andean Geology*, 46(1), 1.
 1063 <https://doi.org/10.5027/andgeoV46n1-3087>
- 1064 Kendall, C. & Caldwell. E.A. (1998) Fundamentals of isotope geochemistry. In: *Isotope Tracers*
 1065 *in Catchment Hydrology* (Eds C. Kendall & J.J. McDonnell), pp. 51-86. Elsevier,
 1066 Amsterdam.
- 1067 Kendall, C., McDonnell, J.J. (1998). *Isotope Tracers in Catchment Hydrology*. 839 pp. Elsevier,
 1068 New York
- 1069 Kesler, S. E., Gruber, P. W., Medina, P. A., Keoleian, G. A., Everson, M. P., & Wallington, T. J.
 1070 (2012). Global lithium resources: Relative importance of pegmatite, brine and other
 1071 deposits. *Ore Geology Reviews*, 48, 55–69.
 1072 <https://doi.org/10.1016/j.oregeorev.2012.05.006>
- 1073 Kinnard, C., Ginot, P., Surazakov, A., MacDonell, S., Nicholson, L., Patris, N., ... Squeo, F. A.
 1074 (2020). Mass Balance and Climate History of a High-Altitude Glacier, Desert Andes of
 1075 Chile. *Frontiers in Earth Science*, 8(February), 1–20.
 1076 <https://doi.org/10.3389/feart.2020.00040>
- 1077 Landerer, F. 2021. TELLUS_GRAC_L3_CSR_RL06_LND_v04. Ver. RL06 v04. PO.DAAC,
 1078 CA, USA. Dataset accessed [2021-02-14] at [https://doi.org/10.5067/TELND-](https://doi.org/10.5067/TELND-3AC64)
 1079 3AC64.Oyarzún, J., & Oyarzún, R. (2011). Sustainable development threats, inter-sector
 1080 conflicts and environmental policy requirements in the arid, mining rich, northern Chile
 1081 territory. *Sustainable Development*, 19(4), 263–274. <https://doi.org/10.1002/sd.441>
- 1082 Landerer, F. W., & Swenson, S. C. (2012). Accuracy of scaled GRACE terrestrial water storage
 1083 estimates. *Water Resources Research*, 48(4), 1–11.
 1084 <https://doi.org/10.1029/2011WR011453>
- 1085 Langenbrunner, B., Pritchard, M. S., Kooperman, G. J., & Randerson, J. T. (2019). Why Does
 1086 Amazon Precipitation Decrease When Tropical Forests Respond to Increasing CO².
 1087 *Earth's Future*, 7(4), 450–468. <https://doi.org/10.1029/2018EF001026>
- 1088 Liu, W., Agusdinata, D. B., & Myint, S. W. (2019). Spatiotemporal patterns of lithium mining
 1089 and environmental degradation in the Atacama Salt Flat, Chile. *International Journal of*
 1090 *Applied Earth Observation and Geoinformation*, 80(January), 145–156.
 1091 <https://doi.org/10.1016/j.jag.2019.04.016>
- 1092 Liu, W., & Agusdinata, D. B. (2020). Interdependencies of lithium mining and communities
 1093 sustainability in Salar de Atacama, Chile. *Journal of Cleaner Production*, 260, 120838.
 1094 <https://doi.org/10.1016/j.jclepro.2020.120838>
- 1095 Liu, Y., Wagener, T., Beck, H. E., & Hartmann, A. (2020). What is the hydrologically effective
 1096 area of a catchment? *Environmental Research Letters*, 15(10), 104024.
 1097 <https://doi.org/10.1088/1748-9326/aba7e5>
- 1098 Masbruch, M. D., Rumsey, C. A., Gangopadhyay, S., Susong, D. D., & Pruitt, T. (2016).
 1099 Analyses of infrequent (quasi-decadal) large groundwater recharge events in the northern

- 1100 Great Basin: Their importance for groundwater availability, use, and management. *Water*
1101 *Resources Research*, 52(10), 7819–7836. <https://doi.org/10.1002/2016WR019060>
- 1102 MEL (Minera Escondida Ltda) (2017). Informe “Plan de Alerta Temprana para el Acuífero
1103 Monturaqui-Negrillar-Tilopozo”. Santiago, Chile
- 1104 McDonnell, J. J. (2017). Beyond the water balance. *Nature Geoscience*, 10(6), 396–396.
1105 <https://doi.org/10.1038/ngeo2964>
- 1106 McKnight, S. V., Boutt, D. F., & Munk, L. A. (2021). Impact of Hydrostratigraphic Continuity
1107 on Brine-to-Freshwater Interface Dynamics: Implications From a Two-Dimensional
1108 Parametric Study in an Arid and Endorheic Basin. *Water Resources Research*, 57(4).
1109 <https://doi.org/10.1029/2020WR028302>
- 1110 Montecino, H. C., Staub, G., Ferreira, V. G., & Parra, L. B. (2016). MONITORING
1111 GROUNDWATER STORAGE IN NORTHERN CHILE BASED ON SATELLITE
1112 OBSERVATIONS AND DATA SIMULATION. *Boletim de Ciências Geodésicas*, 22(1),
1113 1–15. <https://doi.org/10.1590/S1982-21702016000100001>
- 1114 Morales, M. S., Cook, E. R., Barichivich, J., Christie, D. A., Villalba, R., LeQuesne, C., ...
1115 Boninsegna, J. A. (2020). Six hundred years of South American tree rings reveal an
1116 increase in severe hydroclimatic events since mid-20th century. *Proceedings of the*
1117 *National Academy of Sciences*, 117(29), 16816–16823.
1118 <https://doi.org/10.1073/pnas.2002411117>
- 1119 Moran, B. J., Boutt, D. F., & Munk, L. A. (2019). Stable and Radioisotope Systematics Reveal
1120 Fossil Water as Fundamental Characteristic of Arid Orogenic-Scale Groundwater
1121 Systems. *Water Resources Research*, 55(12), 11295–11315.
1122 <https://doi.org/10.1029/2019WR026386>
- 1123 Moran, Brendan J.; Boutt, David F.; McKnight, Sarah V.; Jenckes, Jordan; Munk, Lee Ann;
1124 Corkran, Daniel; and Kirshen, Alexander, "Data for "Relic Groundwater and Mega
1125 Drought Confound Interpretations of Water Sustainability and Lithium Extraction in Arid
1126 Lands"" (2021). Data and Datasets. 145. <https://scholarworks.umass.edu/data/145>
- 1127 Moran, Brendan J., "Fundamental Controls on the Water Cycle in Arid Environments: a
1128 Mechanistic Framework for Spatiotemporal Connectivity Between Hydroclimate and
1129 Groundwaters in the Dry Andes" (2022). Doctoral Dissertations.
1130 https://scholarworks.umass.edu/dissertations_2/1
- 1131 Munk, L.A., Hynek, S.A., Bradley, D.C., Boutt, D.F., Labay, K., Jochens, H., (2016). Lithium
1132 Brines: A Global Perspective, in Verplanck, P.L. and Hitzman, M.W., eds., *Rare Earth*
1133 *and Critical Elements in Ore Deposits. Reviews in Economic Geology* (18), 339–365.
- 1134 Munk, L. A., Boutt, D. F., Hynek, S. A., & Moran, B. J. (2018). Hydrogeochemical fluxes and
1135 processes contributing to the formation of lithium-enriched brines in a hyper-arid
1136 continental basin. *Chemical Geology*, 493, 37–57.
1137 <https://doi.org/10.1016/j.chemgeo.2018.05.013>
- 1138 Munk, L. A., Boutt, D. F., Moran, B. J., McKnight, S. V., & Jenckes, J. (2021). Hydrogeologic
1139 and geochemical distinctions in freshwater-brine systems of an Andean salar.

- 1140 Geochemistry, Geophysics, Geosystems, 22, e2020GC009345.
1141 <https://doi.org/10.1029/2020GC009345>
- 1142 Pabón-Caicedo, J. D., Arias, P. A., Carril, A. F., Espinoza, J. C., Borrel, L. F., Goubanova, K.,
1143 ... Villalba, R. (2020). Observed and Projected Hydroclimate Changes in the Andes.
1144 *Frontiers in Earth Science*, 8(March), 1–29. <https://doi.org/10.3389/feart.2020.00061>
- 1145 Pascale, S., Carvalho, L. M. V, Adams, D. K., Castro, C. L., & Cavalcanti, I. F. A. (2019).
1146 Current and Future Variations of the Monsoons of the Americas in a Warming Climate.
1147 *Current Climate Change Reports*. <https://doi.org/10.1007/s40641-019-00135-w>
- 1148 Pekel, J.-F., Cottam, A., Gorelick, N., & Belward, A. S. (2016). High-resolution mapping of
1149 global surface water and its long-term changes. *Nature*, 540(7633), 418–422.
1150 <https://doi.org/10.1038/nature20584>
- 1151 Pfeiffer, M., Latorre, C., Santoro, C. M., Gayo, E. M., Rojas, R., Carrevedo, M. L., ...
1152 Amundson, R. (2018). Chronology, stratigraphy and hydrological modelling of extensive
1153 wetlands and paleolakes in the hyperarid core of the Atacama Desert during the late
1154 quaternary. *Quaternary Science Reviews*, 197, 224–245.
1155 <https://doi.org/10.1016/j.quascirev.2018.08.001>
- 1156 Pfister, S., Koehler, A., & Hellweg, S. (2009). Assessing the Environmental Impacts of
1157 Freshwater Consumption in LCA. *Environmental Science & Technology*, 43(11), 4098–
1158 4104. <https://doi.org/10.1021/es802423e>
- 1159 Placzek, C. J., Quade, J., & Patchett, P. J. (2013). A 130ka reconstruction of rainfall on the
1160 Bolivian Altiplano. *Earth and Planetary Science Letters*, 363, 97–108.
1161 <https://doi.org/10.1016/j.epsl.2012.12.017>
- 1162 Quade, J., Rech, J. a., Betancourt, J. L., Latorre, C., Quade, B., Rylander, K. A., & Fisher, T.
1163 (2008). Paleowetlands and regional climate change in the central Atacama Desert,
1164 northern Chile. *Quaternary Research*, 69(03), 343–360.
1165 <https://doi.org/10.1016/j.yqres.2008.01.003>
- 1166 Reager, J. T., & Famiglietti, J. S. (2013). Characteristic mega-basin water storage behavior using
1167 GRACE. *Water Resources Research*, 49(6), 3314–3329.
1168 <https://doi.org/10.1002/wrcr.20264>
- 1169 Rech, J. a., Pigati, J. S., Quade, J., & Betancourt, J. L. (2003). Re-evaluation of mid-Holocene
1170 deposits at Quebrada Puripica, northern Chile. *Palaeogeography, Palaeoclimatology,*
1171 *Palaeoecology*, 194(1–3), 207–222. [https://doi.org/10.1016/S0031-0182\(03\)00278-5](https://doi.org/10.1016/S0031-0182(03)00278-5)
- 1172 Ridoutt, B. G., & Pfister, S. (2010). A revised approach to water footprinting to make transparent
1173 the impacts of consumption and production on global freshwater scarcity. *Global*
1174 *Environmental Change*, 20(1), 113–120. <https://doi.org/10.1016/j.gloenvcha.2009.08.003>
- 1175 Rissmann, C., Leybourne, M., Benn, C., & Christenson, B. (2015). The origin of solutes within
1176 the groundwaters of a high Andean aquifer. *Chemical Geology*, 396, 164–181.
1177 <https://doi.org/10.1016/j.chemgeo.2014.11.029>

- 1178 Rivera, J. A., Otta, S., Lauro, C., & Zazulie, N. (2021). A Decade of Hydrological Drought in
 1179 Central-Western Argentina. *Frontiers in Water*, 3(April), 1–20.
 1180 <https://doi.org/10.3389/frwa.2021.640544>
- 1181 Rooyen, J. D., Watson, A. P., Palcsu, L., & Miller, J. A. (2021). Constraining the Spatial
 1182 Distribution of Tritium in Groundwater Across South Africa. *Water Resources Research*,
 1183 57(8). <https://doi.org/10.1029/2020WR028985>
- 1184 Scanlon, B. R., Keese, K. E., Flint, A. L., Flint, L. E., Gaye, C. B., Edmunds, W. M., &
 1185 Simmers, I. (2006). Global synthesis of groundwater recharge in semiarid and arid
 1186 regions. *Hydrological Processes*, 20(15), 3335–3370. <https://doi.org/10.1002/hyp.6335>
- 1187 Schaffer, N., MacDonell, S., Réveillet, M., Yáñez, E., & Valois, R. (2019). Rock glaciers as a
 1188 water resource in a changing climate in the semiarid Chilean Andes. *Regional
 1189 Environmental Change*, 19(5), 1263–1279. <https://doi.org/10.1007/s10113-018-01459-3>
- 1190 Schaller, M. F., & Fan, Y. (2009). River basins as groundwater exporters and importers:
 1191 Implications for water cycle and climate modeling. *Journal of Geophysical Research*,
 1192 114(D4), D04103. <https://doi.org/10.1029/2008JD010636>
- 1193 Schomburg, A. C., Bringezu, S., & Flörke, M. (2021). Extended life cycle assessment reveals the
 1194 spatially-explicit water scarcity footprint of a lithium-ion battery storage.
 1195 *Communications Earth & Environment*, 2(1), 11. <https://doi.org/10.1038/s43247-020-00080-9>
 1196
- 1197 Somers, L. D., & McKenzie, J. M. (2020). A review of groundwater in high mountain
 1198 environments. *WIREs Water*, 7(6). <https://doi.org/10.1002/wat2.1475>
- 1199 Sonter, L. J., Dade, M. C., Watson, J. E. M., & Valenta, R. K. (2020). Renewable energy
 1200 production will exacerbate mining threats to biodiversity. *Nature Communications*, 11(1),
 1201 4174. <https://doi.org/10.1038/s41467-020-17928-5>
- 1202 Steiger, N. J., Smerdon, J. E., Seager, R., Williams, A. P., & Varuolo-Clarke, A. M. (2021).
 1203 ENSO-driven coupled megadroughts in North and South America over the last
 1204 millennium. *Nature Geoscience*, 14(10), 739–744. <https://doi.org/10.1038/s41561-021-00819-9>
 1205
- 1206 Stewart, M. K., Morgenstern, U., Gusyev, M. A., & Maloszewski, P. (2017). Aggregation effects
 1207 on tritium-based mean transit times and young water fractions in spatially heterogeneous
 1208 catchments and groundwater systems, and implications for past and future applications of
 1209 tritium. *Hydrology and Earth System Sciences Discussions*, (October), 1–26.
 1210 <https://doi.org/10.5194/hess-2016-532>
- 1211 Stonestrom, D., & Harrill, R. (2007). Ground-Water Recharge in the Arid and Semiarid
 1212 Southwestern United States—Climatic and Geologic Framework. *Ground-Water
 1213 Resources Program; National Research Program*, (1703), Chapter A. Retrieved from
 1214 http://pubs.er.usgs.gov/thumbnails/usgs_thumb.jpg%5Cnhttp://pubs.usgs.gov/pp/pp1703/
- 1215 Valdivielso, S., Vázquez-Suñé, E., & Custodio, E. (2020). Origin and variability of oxygen and
 1216 hydrogen isotopic composition of precipitation in the Central Andes: A review. *Journal*

- 1217 of Hydrology, 587(December 2019), 124899.
 1218 <https://doi.org/10.1016/j.jhydrol.2020.124899>
- 1219 Vuille, M., & Ammann, C. (1997). Regional snowfall patterns in the high, arid Andes. *Climatic*
 1220 *Change*, 36, 413–423. https://doi.org/10.1007/978-94-015-8905-5_10
- 1221 Wada, Y., Bierkens, M. F. P., de Roo, A., Dirmeyer, P. A., Famiglietti, J. S., Hanasaki, N., ...
 1222 Wheeler, H. (2017). Human–water interface in hydrological modelling: current status and
 1223 future directions. *Hydrology and Earth System Sciences*, 21(8), 4169–4193.
 1224 <https://doi.org/10.5194/hess-21-4169-2017>
- 1225 Wang, J., Song, C., Reager, J. T., Yao, F., Famiglietti, J. S., Sheng, Y., ... Wada, Y. (2018).
 1226 Recent global decline in endorheic basin water storages. *Nature Geoscience*, 11(12), 926–
 1227 932. <https://doi.org/10.1038/s41561-018-0265-7>
- 1228 Wiese, D. N., Landerer, F. W., & Watkins, M. M. (2016). Quantifying and reducing leakage
 1229 errors in the JPL RL05M GRACE mascon solution. *Water Resources Research*, 52(9),
 1230 7490–7502. <https://doi.org/10.1002/2016WR019344>
- 1231 Zipper, S. C., Jaramillo, F., Wang-Erlandsson, L., Cornell, S. E., Gleeson, T., Porkka, M., ...
 1232 Gordon, L. (2020). Integrating the Water Planetary Boundary With Water Management
 1233 From Local to Global Scales. *Earth’s Future*, 8(2).
 1234 <https://doi.org/10.1029/2019EF001377>
- 1235 **References from Supporting Information**
- 1236 Clarke, W.B., Jenkins, W.J., Top, Z. (1976). Determination of tritium by mass spectrometric
 1237 measurement of ³He. *Int. J. Appl. Radiat. Isot.* 27 (9), 515e522.
- 1238 Condom, T., Martínez, R., Pabón, J. D., Costa, F., Pineda, L., Nieto, J. J., ... Villacis, M. (2020).
 1239 Climatological and Hydrological Observations for the South American Andes: In situ
 1240 Stations, Satellite, and Reanalysis Data Sets. *Frontiers in Earth Science*, 8(April), 1–20.
 1241 <https://doi.org/10.3389/feart.2020.00092>
- 1242 Dubey, S., Gupta, H., Goyal, M. K., & Joshi, N. (2021). Evaluation of precipitation datasets
 1243 available on Google earth engine over India. *International Journal of Climatology*,
 1244 41(10), 4844–4863. <https://doi.org/10.1002/joc.7102>
- 1245 Eshel, G., Araus, V., Undurraga, S., Soto, D. C., Moraga, C., Montecinos, A., ... Gutiérrez, R. A.
 1246 (2021). Plant ecological genomics at the limits of life in the Atacama Desert. *Proceedings*
 1247 *of the National Academy of Sciences*, 118(46), e2101177118.
 1248 <https://doi.org/10.1073/pnas.2101177118>
- 1249 Gorelick, N., Hancher, M., Dixon, M., Ilyushchenko, S., Thau, D. and Moore, R. (2017) Google
 1250 earth engine: planetary-scale geospatial analysis for everyone. *Remote Sensing of*
 1251 *Environment*, 202, 18–27. <https://doi.org/10.1016/j.rse.2017.06.031>.
- 1252 Hipel, K.W. and McLeod, A.I. (1994), *Time Series Modelling of Water Resources and*
 1253 *Environmental Systems*. New York: Elsevier Science.

- 1254 Hirsch, R. M., Slack, J. R., and Smith, R. A. (1982), Techniques of trend analysis for monthly
 1255 water quality data, *Water Resour. Res.*, 18(1), 107– 121,
 1256 doi:10.1029/WR018i001p00107.
- 1257 Hussain et al., (2019). pyMannKendall: a python package for non parametric Mann Kendall
 1258 family of trend tests. *Journal of Open Source Software*, 4(39), 1556,
 1259 <https://doi.org/10.21105/joss.01556>
- 1260 Jordan, T. E., Mpodozis, C., Muñoz, N., Blanco, N., Pananont, P., & Gardeweg, M. (2007).
 1261 Cenozoic subsurface stratigraphy and structure of the Salar de Atacama Basin, northern
 1262 Chile. *Journal of South American Earth Sciences*, 23(2–3), 122–146.
 1263 <https://doi.org/10.1016/j.jsames.2006.09.024>
- 1264 Lucas, L., & Unterweger, M. (2000). Comprehensive review and critical evaluation of the half-
 1265 life of tritium. *Journal of Research of the National Institute of Standards and Technology*,
 1266 105(4), 541–549. <https://doi.org/10.6028/jres.105.043>
- 1267 MEL (Minera Escondida Ltda) (2017). Informe “Plan de Alerta Temprana para el Acuífero
 1268 Monturaqui-Negrillar-Tilopozo”. Santiago, Chile
- 1269 NASA. (2000). Measuring Vegetation, Normalized Difference Vegetation Index (NDVI)
 1270 [https://www.usgs.gov/core-science-systems/eros/phenology/science/ndvi-foundation-
 1271 remote-sensing-phenology?qt-science_center_objects=0#qt-science_center_objects](https://www.usgs.gov/core-science-systems/eros/phenology/science/ndvi-foundation-remote-sensing-phenology?qt-science_center_objects=0#qt-science_center_objects).
- 1272 Rubilar, J., Martínez, F., Arriagada, C., Becerra, J., & Bascuñán, S. (2018). Structure of the
 1273 Cordillera de la Sal: A key tectonic element for the Oligocene-Neogene evolution of the
 1274 Salar de Atacama basin, Central Andes, northern Chile. *Journal of South American Earth
 1275 Sciences*, 87, 200–210. <https://doi.org/10.1016/j.jsames.2017.11.013>
- 1276 Salio, P., Hobouchian, M. P., García Skabar, Y., & Vila, D. (2015). Evaluation of high-
 1277 resolution satellite precipitation estimates over southern South America using a dense
 1278 rain gauge network. *Atmospheric Research*, 163, 146–161.
 1279 <https://doi.org/10.1016/j.atmosres.2014.11.017>
- 1280 Schween, J. H., Hoffmeister, D., & Löhnert, U. (2020). Filling the observational gap in the
 1281 Atacama Desert with a new network of climate stations. *Global and Planetary Change*,
 1282 184(May 2019), 103034. <https://doi.org/10.1016/j.gloplacha.2019.103034>
- 1283 Tucker C.J. (1979) Red and photographic infrared linear combinations monitoring vegetation.
 1284 *Journal of Remote Sensing Environment*, 8(2), 127-150. doi:10.1016/0034-
 1285 4257(79)90013-0
- 1286 USGS (U.S. Geological Survey) (2018). NDVI, the Foundation for Remote Sensing Phenology.
 1287 [https://www.usgs.gov/core-science-systems/eros/phenology/science/ndvi-foundation-
 1288 remote-sensing-phenology?qt-science_center_objects=0#qt-science_center_objects](https://www.usgs.gov/core-science-systems/eros/phenology/science/ndvi-foundation-remote-sensing-phenology?qt-science_center_objects=0#qt-science_center_objects)
- 1289 USGS (U.S. Geological Survey) (2022). Mineral commodity summaries 2022: U.S. Geological
 1290 Survey, 202 p., <https://doi.org/10.3133/mcs2022>.